Biomaterials Science

REVIEW

View Article Online
View Journal | View Issue

Check for updates

Cite this: *Biomater. Sci.*, 2018, **6**, 915

Bioinks for 3D bioprinting: an overview

P. Selcan Gungor-Ozkerim,†[a,b,c] Ilyas Inci,†[a,b] Yu Shrike Zhang,†[a,b,d] Ali Khademhosseini[a,b,d,e,f,g,h,i,j] and Mehmet Remzi Dokmeci*[a,b,d,e,f]

Received 22nd August 2017,
Accepted 12th January 2018

DOI: 10.1039/c7bm00765e

rsc.li/biomaterials-science

Bioprinting is an emerging technology with various applications in making functional tissue constructs to replace injured or diseased tissues. It is a relatively new approach that provides high reproducibility and precise control over the fabricated constructs in an automated manner, potentially enabling high-throughput production. During the bioprinting process, a solution of a biomaterial or a mixture of several biomaterials in the hydrogel form, usually encapsulating the desired cell types, termed the bioink, is used for creating tissue constructs. This bioink can be cross-linked or stabilized during or immediately after bioprinting to generate the final shape, structure, and architecture of the designed construct. Bioinks may be made from natural or synthetic biomaterials alone, or a combination of the two as hybrid materials. In certain cases, cell aggregates without any additional biomaterials can also be adopted for use as a bioink for bioprinting processes. An ideal bioink should possess proper mechanical, rheological, and biological properties of the target tissues, which are essential to ensure correct functionality of the bioprinted tissues and organs. In this review, we provide an in-depth discussion of the different bioinks currently employed for bioprinting, and outline some future perspectives in their further development.

Published on 01 2018. Downloaded on 22.5.2025 22:31:12.

1. Introduction

Biofabrication is an emerging research area and includes the creation of tissue constructs with a hierarchical architecture. Conventional biofabrication techniques include, for example, particulate leaching, freeze-drying, electrospinning, and micro-engineering.[1] Although these techniques can all generate three-dimensional (3D) structures with a wide range of biomaterials, they typically possess limited reproducibility and versatility in their fabrication procedures. The most recent definition of biofabrication is the generation of biologically functional products in an automated manner with structural organization by using bioactive molecules, living cells, and cell aggregates, such as micro-tissues, biomaterials, or hybrid cell-material constructs *via* bioassembly or bioprinting, and subsequent tissue maturation processes.[2] More recently, 3D bioprinting has emerged as a novel biofabrication method, offering significantly improved control over the architecture of the fabricated tissue constructs with high reproducibility endowed by the automated deposition process.[3–5] Essentially, bioprinting allows for the fabrication of 3D tissue constructs with pre-programmed structures and geometries containing biomaterials and/or living cells (together termed the bioink) by synchronizing the bioink deposition/cross-linking with the motorized stage movement. Although bioprinting is still in its early developmental stages, its versatility has continued to accelerate the applications in tissue engineering.[6]

The main 3D bioprinting modalities (Fig. 1),[3] in general can be classified as: laser-assisted bioprinting (LaBP), inkjet bioprinting/droplet bioprinting, and extrusion-based bioprinting.[7–10] In addition, the use of multi-head deposition systems (MHDSs) allows the simultaneous or subsequent printing of multiple materials. Besides, there are several custom-made bioprinting systems developed with various application-specific functions.[7–10] In these methods, 3D con-

[a]*Biomaterials Innovation Research Center, Division of Engineering in Medicine, Department of Medicine, Brigham and Women's Hospital, Harvard Medical School, Cambridge, MA 02139, USA*
[b]*Harvard-MIT Division of Health Sciences and Technology, Massachusetts Institute of Technology, Cambridge, MA 02139, USA.*
E-mail: mdokmeci@rics.bwh.harvard.edu
[c]*Department of Biomedical Engineering, Faculty of Engineering and Natural Sciences, Biruni University, Istanbul 34010, Turkey*
[d]*Wyss Institute for Biologically Inspired Engineering, Harvard University, Boston, MA 02115, USA*
[e]*Department of Radiology, David Geffen School of Medicine, University of California-Los Angeles, Los Angeles, CA 90095, USA*
[f]*Center for Minimally Invasive Therapeutics (C-MIT), University of California-Los Angeles, Los Angeles, CA 90095, USA*
[g]*Department of Bioindustrial Technologies, College of Animal Bioscience and Technology, Konkuk University, Seoul 143-701, Republic of Korea*
[h]*Center for Nanotechnology, King Abdulaziz University, Jeddah 21569, Saudi Arabia*
[i]*Department of Bioengineering, Department of Chemical and Biomolecular Engineering, Henry Samueli School of Engineering and Applied Sciences, University of California-Los Angeles, Los Angeles, CA 90095, USA*
[j]*California NanoSystems Institute (CNSI), University of California-Los Angeles, Los Angeles, CA 90095, USA*
†These authors contributed equally to this work.

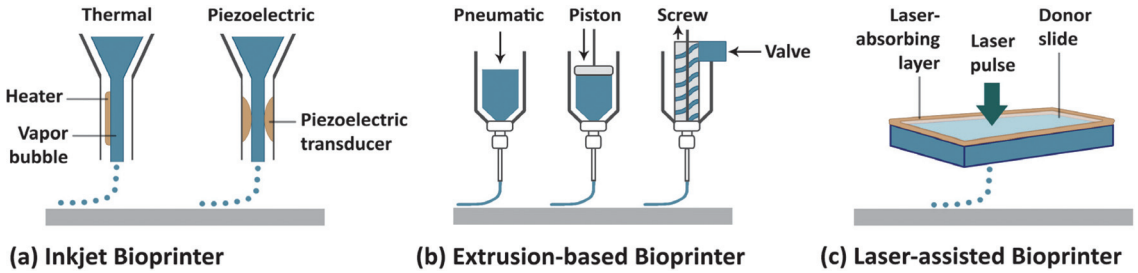

Fig. 1 Schematic representation of the main 3D bioprinting technologies. (a) Inkjet/droplet bioprinting. (b) Extrusion-based bioprinting. (c) Laser-assisted bioprinting.[3] Reproduced with permission Copyright Nature Publishing Group, 2014.

Published on 01 2018. Downloaded on 22.5.2025 22:31:12.

structs are programmed in a computer-aided design/computer-aided manufacturing (CAD/CAM) system. In all of these different bioprinting strategies, however, the bioinks are an essential component, and are cross-linked or stabilized during or immediately after the bioprinting to create the final shapes of the intended tissue constructs. The selection of the bioink depends on the specific application (*e.g.*, target tissue) and the type of cells as well as the bioprinter to be used. While the field has seen significant development in the bioprinting modalities (reviewed elsewhere),[7–10] their applications have been limited by the lack of appropriate bioinks, which both need to meet the requirements for bioprinting and to have the proper bioactivity of the different cell types.

An ideal bioink should possess the desired physicochemical properties, such as proper mechanical, rheological, chemical, and biological characteristics.[11] These properties should lead to: (i) the generation of tissue constructs with adequate mechanical strength and robustness, while retaining the tissue-matching mechanics, preferably in a tunable manner; (ii) adjustable gelation and stabilization to aid the bioprinting of structures with high shape fidelity; (iii) biocompatibility and, if necessary, biodegradability mimicking the natural microenvironment of the tissues; (iv) suitability for chemical modifications to meet tissue-specific needs; and (v) the potential for large-scale production with minimum batch-to-batch variations.[12] Since determining the optimal cell-laden bioink formulation is the vital step toward successful bioprinting, to date, various natural and synthetic biomaterials with specific features have been utilized as bioinks.[13] Moreover, standardized bioink formulations are urgently needed that allow for their use in different bioprinting applications.

The goal of this review is therefore to present an in-depth overview of the state of the art in existing bioinks. The review includes both natural and synthetic biomaterials used either alone or in combination, and in certain cases, multicellular spheroids used as bioinks (Table 1). Those studies in which biopolymers are printed without embedded cells and those where the cells are seeded post-printing are excluded from the review, and only bioinks that contain cells are discussed. We first describe natural bioinks and then move on to synthetic bioinks and multicellular spheroids, followed by several commercial bioinks, where the main advantages and drawbacks of

P. Selcan Gungor-Ozkerim

Selcan Gungor Ozkerim is a bioengineer and holds an MSc in Biomedical Engineering. Her PhD was based on designing complex 3D tissue scaffolds for tissue engineering purposes. She developed a novel multilayered nanofibrous scaffold system by using various polymeric biomaterials in combination with controlled release systems. She worked at Harvard – Massachusetts Institute of Technology (MIT) in the Health Sciences & Technology (HST) division as a postdoctoral research fellow and studied the 3D bioprinting of cell-laden tissue constructs. She generated viable and perfusable functional vascular constructs that could be utilized for the vascularization of various tissue scaffolds.

Ilyas Inci

Ilyas Inci received his Ph.D in Bioengineering at Hacettepe University in Turkey. His Ph.D study was on the effect of cryogel scaffolds for calvarial defect repair. After his Ph.D, he worked as a post-doctoral research fellow in Sabanci University in Turkey and then he attended Harvard-Massachusetts Institute of Technology (MIT), Health Sciences and Technology division to do research on tissue engineering as a post-doctoral research fellow. His research interests mainly focus on using biocompatible scaffolds to develop therapeutic methods in tissue engineering and analyzing the effects of applied tissue engineering methods on molecular signaling during tissue regeneration.

 This journal is © The Royal Society of Chemistry 2018

Published on 01 2018. Downloaded on 22.5.2025 22:31:12.

each category are discussed. We subsequently provide a short section to elaborate on some of the new bioink formulation strategies that are not mentioned in the preceding sections. We finally conclude with future perspectives on the remaining challenges associated with the current bioinks and the further need for standardization.

2. Hydrogel-based bioinks

Hydrogels have numerous attractive features for use as tissue scaffolds. For example, they are biocompatible and typically biodegradable, and a majority of them possess specific cell-binding sites that are desirable for cell attachment, spreading, growth, and differentiation. In addition, some of these biomaterials in their modified forms can be readily photocross-linked.[14] Hydrogel biomaterials, including alginate, gelatin, collagen, fibrin/fibrinogen, gellan gum, hyaluronic acid (HA), agarose, chitosan, silk, decellularized extracellular matrix (dECM), poly(ethylene glycol) (PEG), and Pluronic, and their use as bioinks will be discussed in the following section.

2.1. Protein-based bioinks

Collagen is the main structural protein in the extracellular matrix (ECM) of mammalian cells. Collagen thus possesses tissue-matching physicochemical properties, together with superior *in vitro*/*in vivo* biocompatibility, and has been widely used in biomedical applications.[15] Koch *et al.* used collagen as a bioink formulation with encapsulated keratinocytes and fibroblasts and bioprinted multilayer 3D skin tissue constructs *via* LaBP.[16] They investigated the viability and morphological functions of both cell types following bioprinting. Their findings demonstrated the presence of intercellular communications between different cell types and suggested that the fabricated skin grafts had tissue-specific functions, which are promising for fabricating complex multicellular tissue constructs. The same group further evaluated the *in vivo* applications of these constructs and demonstrated the formation of 3D skin-like tissue *via* proliferation and proper differentiation of the cells.[17] Another study also utilized a collagen bioink for skin tissue engineering and created mature tissues with distinct cell layers.[18] Moon *et al.* developed a valve-based droplet ejector system to bioprint smooth muscle cells (SMCs)-laden collagen droplets, which formed line patterns with layer-by-layer deposition and demonstrated uniform cell seeding with controlled resolution.[19] In another study, the differentiation potential of bioprinted mesenchymal stem cells (MSCs) was investigated.[20] Here, MSCs were encapsulated in collagen alone or collagen–agarose blend bioink and were bioprinted using an extrusion-based platform. The collagen-only matrix supported the spreading of the cells following printing, in contrast to the behavior of the cells in the hybrid matrix made with agarose, which kept its structural integrity but did not allow cell spreading. The results revealed that the anisotropic soft collagen-rich matrices were better suited for osteogenesis, whereas the isotropic stiff agarose-rich matrices supported adipogenesis of the bioprinted 3D constructs. Collagen may also be combined with alginate for use as a composite bioink. Also, preosteoblasts and human adipose tissue-derived stem cells (ASCs) were encapsulated in this bioink to bioprint 3D porous cellular blocks.[11] Here, the cells were first cultured on a collagen gel and then the cell-laden collagen gel was combined with alginate. The results showed that the osteogenic potential of the collagen-alginate bioink was higher than the one with alginate alone. Moreover, hepatic lineage differentiation of the ASCs was also achieved in the bioprinted blocks, implying that

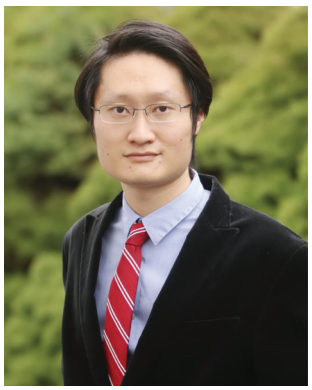

Yu Shrike Zhang

Yu Shrike Zhang received his Ph.D. from Georgia Institute of Technology in the Wallace H. Coulter Department of Biomedical Engineering in 2013. He is currently a Faculty and Associate Bioengineer in the Division of Engineering in Medicine at the Brigham and Women's Hospital, Harvard Medical School. Dr Zhang's research is focused on innovating medical engineering technologies to recreate functional biomimetic tissues and tissue models, including biomaterials, bioprinting, organs-on-chips, medical devices, biomedical imaging, and biosensing. He is actively collaborating with a multidisciplinary team encompassing biomedical, mechanical, electrical, and computer engineers as well as biologists and clinicians to ultimately translate these cutting-edge technologies into clinics.

Ali Khademhosseini

Ali Khademhosseini is the Levi Knight Professor of Bioengineering, Chemical Engineering and Radiology at the University of California-Los Angeles (UCLA). He is the Founding Director of the Center for Minimally Invasive Therapeutics (C-MIT) at UCLA and the Associate Director of the California NanoSystems Institute. Previously, he was a Professor of Medicine at Harvard Medical School. He is recognized as a leader in combining micro- and nano-engineering approaches with advanced biomaterials for regenerative medicine applications and has authored ~500 journal papers (H-index >98 & >35 000 citations). He is a fellow of AIMBE, BMES, RSC, FBSE, and AAAS. Read more at: http://www.tissueeng.net/.

Published on 01 2018. Downloaded on 22.5.2025 22:31:12.

this new bioink could be used in various tissue engineering applications. Collagen is also widely used as a biopaper in bioprinting applications. Biopaper is the substrate used in bioprinting and is the analog of the media used in standard printing processes and it is commonly referred to the hydrogel surface on which the cell-laden bioink or cell spheroids can be bioprinted.[21–23]

Gelatin is produced by the denaturation of collagen.[24] It can be derived from bones, tendons, or skins of animals *via* acidic or basic hydrolysis. Its solution is thermosensitive and can form a hydrogel at lower temperatures in a concentration-dependent manner, and consequently it is one of the most widely used natural polymers for many biomedical applications. Some of the superior advantages of gelatin include biocompatibility, biodegradability, low antigenicity, inclusion of intrinsic Arg-Gly-Asp (RGD) motifs, accessible active groups, absence of harmful byproducts, ease of processing, and low cost.[25–27] All of these properties, and especially its cellular affinity, make it a versatile material for applications in tissue engineering and bioprinting. For bioprinting applications, gelatin with a wide range of concentrations has been used as a bioink material and/or as a composite with other polymers. In addition, its modified forms, which can be chemically cross-linked, have also been adapted for bioprinting, such as gelatin methacryloyl (GelMA).[28]

Zhang *et al.* used gelatin–alginate composite bioinks to encapsulate myoblasts and investigated the mechanical properties of the bioprinted soft tissue constructs.[29] By using a dual-nozzle system, they bioprinted 3D filaments with different structural configurations, such as layers with specific angles. The process consisted of a two-step cross-linking procedure; the physical cross-linking of gelatin at a low temperature during bioprinting and ionic cross-linking of the alginate with Ca^{2+} ions following the bioprinting step. They observed that the mechanical strength of the cell-laden constructs decreased during the culture period but the low-porosity and the angled geometry of the structures supported their mechanical durability. Although bioprinting at low temperatures resulted in a drastic decrease in cell viability during the first few days, cell proliferation increased over culture. In another study, a gelatin–alginate composite bioink was used for bioprinting hard tissue constructs.[30] The authors reported that human osteosarcoma cells remained in a non-proliferating state within this composite bioink matrix, so they proposed filling the construct with an agarose overlay following bioprinting. Moreover, they added [polyphosphate (polyp). Ca^{2+}-complex] into the overlay for better mineral deposition. This combined system significantly improved both the cellular proliferation and mechanical properties of the cell-laden constructs, indicating that this system could be extended for other tissue engineering applications by adapting it for specific tissue needs. Another study utilized gelatin–alginate hydrogels for bioprinting cell-laden aortic valve conduits designed from micro-computed tomography images.[31] They simultaneously bioprinted encapsulated SMCs in the valve root part and valve leaflet interstitial cells in the leaflet part of the constructs in line with their anatomical regions by using an extrusion-based bioprinter. The bioprinted constructs were close to clinical dimensions and were cross-linked in a $CaCl_2$ solution post-printing. It was noted that the optimal ratio of the gelatin and alginate combination in the blend was crucial for the printing quality for enabling proper cell growth, spreading, and phenotypic maturation. Using the same bioprinting system, Wüst *et al.* fabricated 3D tubular constructs using a composite hydrogel with tunable properties.[32] Additionally, they used syringe tip heaters to control the temperature of the bioink, which prevented clogging and hence improved the bioprinting process. They supplemented the gelatin/alginate bioink with hydroxyapatite (HAp), which is an osteoinductive agent with numerous applications in bone tissue engineering.

Due to its thermoresponsive property, gelatin can be tuned and physically cross-linked during bioprinting by thermal gelation, which helps to maintain the shapes of the bioprinted structures. However, temperature-induced gelation is typically slow and unstable. To address this problem, gelatin has been further modified with photopolymerizable methacryloyl groups, enabling covalent cross-linking by UV light under mild conditions following the bioprinting process.[33–37] This functionalized form of gelatin, namely GelMA, is a promising bioink material because its cross-linking density can be easily controlled during methacryloyl group activation or during photopolymerization, which determines the physicochemical properties of the final construct. In bioprinting, since preservation of the integrity and mechanical strength of the bioprinted constructs are two of the most important criteria, GelMA is a suitable material for meeting these requirements. Our group reported a strategy for bioprinting cell-laden GelMA bioinks by using an extrusion-based bioprinter.[38] Various GelMA and cell concentrations and different UV exposure times were explored to evaluate the printability of cell-laden

Mehmet Remzi Dokmeci

Mehmet Remzi Dokmeci is an Associate Adjunct Professor of Radiology at the University of California-Los Angeles (UCLA). Previously, he was an Instructor of Medicine at Brigham and Women's Hospital, Harvard Medical School. He has also worked at Corning-Intellisense, a MEMS foundry and was a faculty member in the Department of Electrical and Computer Engineering at Northeastern University. Dr Dokmeci has long standing expertise in micro- and nanoscale sensors and devices and related applications to biomedical devices, organs on a chip, regenerative medicine and implantable biosensors. He has written over 116 journal articles, 110 conference publications, 4 book chapters, and has 4 patents.

This journal is © The Royal Society of Chemistry 2018

Published on 01 2018. Downloaded on 22.5.2025 22:31:12.

Table 1 Summary of various bioinks used to date

Natural biomaterial-based bioinks

Biomaterial	Bioprinting method	Cell type	Target tissue	Cellular response	Ref.
Alginate	Extrusion-based printing	Cartilage progenitor cells (CPCs)	Vascular	89% cell viability, after 12 h to 72 h incubation	59
	Extrusion-based printing	CPCs	Vascular	95% cell viability, up to day 7; better differentiation	60
	Extrusion-based printing	Human umbilical vein SMCs	Vascular	High proliferation up to day 7; ECM formation	54
	Extrusion-based printing	L929 mouse fibroblasts	Vascular	>90% cell viability in day 1, >70% cell viability up to day 7	61
	Laser-assisted cell printing	NIH-3T3 fibroblasts		Cell viability after 24 h decreased with increased gelation, alginate, Ca^{2+} or laser exposure	62
	Laser-assisted cell printing	Rabbit carcinoma cell line B16 and human umbilical vein endothelial cells (HUVECs) cell line Eahy926		High cell density and cell level organization	63
	Laser-assisted cell printing	Human breast cancer cells		85% or higher cell viability up to day 5	64
	Extrusion-based printing	NIH-3T3 mouse fibroblasts		Microscopic evaluation: similar viability between day 1 and day 7	65
	Extrusion-based printing	ASCs		>90% cell viability on day 9	66
	MHDS	Rat heart endothelial cells		Around 80% cell viability up to day 21	9
	MHDS	Rat adrenal medulla endothelial cells		Increased printing pressure decreased cell viability at around 40%	67
	MHDS	Liver cells, human hepatic carcinoma cells cell line HepG2	Liver	Enhanced metabolic drug conversion	68
	Inkjet bioprinting	NIH-3T3 mouse fibroblasts	Vascular	>80% cell viability in 72 h	71
	Inkjet bioprinting	NIH-3T3 mouse fibroblasts		Increasing cell concentration increased droplet breakup time	72
	Extrusion-based printing	Human ASCs (hASCs)		Proliferation, spreading and structure integrity up to 8 days of incubation	55
Gelatin	Cell assembler	C2C12 mouse myoblasts		55% cell viability 2 h after printing and increased up to day 4	29
	Rapid prototyping with 3D Bioplotter	Human osteogenic sarcoma cells SaOS-2		Non-proliferating state; addition of [polyp.Ca^{2+} complex] and agarose improved proliferation	30
	Extrusion-based printing	Aortic root sinus SMCs and aortic valve leaflet interstitial cells	Aortic valve	>80% cell viability on day 7; good spreading and phenotype retention	31
	Extrusion-based printing	HepG2 and NIH-3T3 cells	Vascular	>80% cell viability up to day 8 after printing	38
	MHDS	HUVECs and human neonatal dermal fibroblasts	Vascular	Around 70% cell viability on day 0; >80% cell viability on day 7 after printing	39
	Extrusion-based printing	MSCs	Cartilage	Cell viability of all the bioinks (agarose, alginate, GelMA and BioINK) were around 80%	42
	Extrusion-based printing	ACPCs, MSCs, chondrocytes	Cartilage	Cell viabilities were around 75% and 90% at days 1 and 14 after bioprinting, respectively	43
Collagen	Laser-assisted bioprinting	NIH-3T3 fibroblasts and human keratinocyte cell line (HaCaT)	Skin	Intercellular interactions between different cell types; viability up to 10 days	16
	Laser-assisted bioprinting	NIH-3T3 fibroblasts and HaCaT	Skin	Proliferation and differentiation profiles were similar to native tissue	17
	Robotic dispensing	Fibroblasts (HFF-1) and HaCaT	Skin	Matured distinct multiple cell layers on day 14; >80% cell viability up to day 7	18
	Droplet ejector printing	Bladder SMCs		>90% cell viability following printing; proliferation up to 14 days; successful cell patterning	19
	Custom-made drop-on-demand bioprinting	MSCs	Bone	>95% cell viability on day 21; osteogenic differentiation	20
	Extrusion-based printing	hASCs and preosteoblasts (MC3T3-E1)	Bone and liver	>85% cell viability on day 1, proliferation up to day 7; higher osteogenic activity and hepatogenic differentiation	11

Published on 01 2018. Downloaded on 22.5.2025 22:31:12.

Table 1 *(Contd.)*

Natural biomaterial-based bioinks

Biomaterial	Bioprinting method	Cell type	Target tissue	Cellular response	Ref.
Fibrinogen/ fibrin	Custom-made inkjet bioprinter	Not specified		Good expansion and proliferation up to day 7	46
	Inkjet printing	Rabbit articular chondrocytes	Cartilage	>80% cell viability up to day 7; tissue-specific ECM formation	47
	Laser-assisted bioprinting	ASCs and endothelial colony-forming cells	Vascular	Interaction between different cells in different layers	48
Gellan gum	Extrusion-based printing	MC3T3		Addition of gellan gum did not affect cell viability	77
	Extrusion-based printing	Equine chondrocytes and MSCs		75–86% viability after 1–3 days post printing	80
	Extrusion-based printing	Rat bone marrow MSCs	Bone/ cartilage	Microcarriers supported cell viability, spread and osteogenic differentiation	81
	Extrusion-based, hand-held bioprinting	Primary neural cells	Brain	>70% viability up to day 5; RGD improved cell growth and network formation	79
Silk	Robotic dispensing	BALB/3T3 mouse fibroblasts		Average viability of 71% after 48 h of incubation	51
	MHDS	Human nasal inferior turbinate-derived MSCs		Hydrogel cross-linking with mushroom tyrosinase supported chondrogenic and adipogenic differentiation, cross-linking with sonication supported osteogenic differentiation	52
Hyaluronic acid	Extrusion-based printing	Chondrocyte, osteoblast	Osteo-chondral	Osteoblasts encapsulated in collagen-1 hydrogel showed higher amount of osteogenic marker than osteoblasts within HA; chondrocytes cultured on HA hydrogels showed higher expression of chondrogenic marker than chondrocytes cultured on collagen-1	85
	Commercial multi-material bioprinter	Human aortic valvular interstitial cells	Heart valve	Cell viability was >90% for the encapsulated cells	41
	Dual syringe deposition tool	HepG2, human intestinal epithelial cells (Int-407), NIH-3T3 fibroblasts		Cells attached only to the parts of hydrogels containing a blend of GeMA and HAMA and they did not attach to only HAMA parts	40
	Extrusion-based printing	HepG2, Int-407, NIH-3T3 fibroblasts		Cell viability was more than 95% at day 3 and at day 7	86
	Pneumatic dispensing	Chondrocytes	Cartilage	After 3 days, cell viability of chondrocytes seeded on printed GelMA and on GelMA-HA scaffolds were around 73% and 82% respectively	27
	Bioprinter with a temperature control unit and a UV light source	Bovine chondrocytes		Embedding the cells in the bioink caused cell death and after removal of HA-pNIPAAM, there was a high cell viability due to the improved diffusion	87
Dextran	Pneumatic dispensing	Equine chondrocytes		HA-dexHEMA preparations showed appropriate viscoelastic and pseudoplastic behaviors	89
Agarose	Droplet generation by nitrogen pressure and valve opening	Rat bladder SMCs		Cell viabilities were approximately 95%	19
	Extrusion-based bioprinting	SaOS2		Application of poly-P.Ca^{2+} increased cell proliferation	30
	Extrusion-based bioprinting	Human MG-63 osteosarcoma cells, mouse fibroblasts		Cell viabilities on day 1, at 4 days and at 7 days after fabrication were 96%, 99% and 97% respectively	91
	Bioprinting with a valve ejector	NIH-3T3 murine fibroblasts		Cells stayed alive for 2 weeks in the scaffolds	93
	Extrusion-based bioprinting with a high-density fluid	Human MSCs (hMSCs), MG-63 osteosarcoma cells		Cells were viable 24 h after bioprinting and after 21 days in culture	92
Agarose/ chitosan	Extrusion-based bioprinting	hMSCs		Cell viabilities ≥95%; on day 21; in collagen matrix, cells differentiate into osteogenic tissue and in agarose matrix, they differentiate into adipogenic tissue	20

This journal is © The Royal Society of Chemistry 2018

Published on 01 2018. Downloaded on 22.5.2025 22:31:12.

Table 1 *(Contd.)*

Natural biomaterial-based bioinks

Biomaterial	Bioprinting method	Cell type	Target tissue	Cellular response	Ref.
Hydroxy-apatite	Inkjet bioprinting	hMSCs	Bone	In HAp used group, expression of collagen and ALP were the highest	111
	Pneumatic dispensing	Goat multipotent stromal cells	Bone	In the fast release group, osteocalcin expression was lower than the slow release group; results revealed that the release speed did not change bone volume significantly	104
	3D bioprinting with a heatable nozzle	hMSCs	Bone	Cell viability was 85% after 3 days of *in vitro* culture	32
	Laser-assisted bioprinting	Human osteoprogenitor cells	Bone	Cell viability and proliferation did not change up to 15 days	141
	Laser-assisted bioprinting	Human endothelial cells EA.hy926		Droplets were obtained with 70 μm in diameter with five to seven living cells per droplet	142
De-cellularized matrix based bioinks	Bioprinting with plunger-based dispensing system	hASCs, human inferior turbinate tissue-derived MSCs, L6 rat myoblasts	Adipose/ heart/ cartilage	High cell survival, cell-line-specific gene expression and specific ECM formation in printed tissue constructs	99
	Dispensing system based bioprinting	ASCs	Adipose	After decellularization, remaining DNA content was 3%	100
	Extrusion-based bioprinting	Primary human hepatocytes, primary human stellate cells, primary human Kupffer cells	Liver	Printed tissue construct was functional as seen from production of detectable levels of albumin and urea	101
Growth factor based bioinks	Inkjet bioprinting	C2C12		Cells on the printed BMP-2 samples showed a significant increase in ALP expression; on the control and printed FGF-2 samples no noticeable ALP expression was observed	146
	Inkjet bioprinting	C2C12		Histological analysis showed human acellular dermis alone did not result in bone formation; bone formation was observed on the BMP-2-printed construct parts	121
Matrigel	Pneumatic dispensing system	Endothelial progenitor cells	Vascular	Alginate improved printing; degradation was increased and formation of vessel-like structures were decreased	106
	Extrusion-based printing	HepG2, human mammary epithelial of the cell line (M10)	Liver	Cells were viable 48 h after printing	103
	Laser-assisted bioprinting	Rabbit carcinoma cell line (B16), HUVECs		Cells were viable 24 h after printing	63
	Pneumatic dispensing	Goat multipotent stromal cells	Bone	In the fast release group osteocalcin expression was lower than the slow release group; micro-CT results revealed that release speed did not change bone volume significantly	104
	Inkjet bioprinting	Human alveolar epithelial type II cell line A549, hybrid human cell line EA.hy926	Lung	Cell viability >95% for epithelial cells and co-cultures; ≥86% for endothelial cells	105
	Extrusion-based printing	Human MSCs, human H1 embryonic stem cells, Caco2 cells, HUVECs, human adult dermal fibroblasts, human adult keratinocytes	Gastro-intestinal/ skin	Subcutaneous implantation of hydrogels revealed very low immune response without capsule formation for 2 months	12

Synthetic-biomaterials-based bioinks

Biomaterial	Bioprinting method	Cell type	Target tissue	Cellular response	Ref.
PCL	Extrusion-based printing	Chondrocyte, osteoblast	Osteo-chondral tissue	Osteoblasts in collagen-1 hydrogel showed higher amount of osteogenic marker than osteoblasts in HA; chondrocytes in HA hydrogels showed higher expressions of chondrogenic markers than chondrocytes cultured in collagen-1	85
	Inkjet bioprinting	Rabbit chondrocytes	Cartilage	Cell viability was 80% one week after printing; after 8 weeks, large amount of cartilage ECM formation on printed constructs	47
	MHDS	Human nasal septal chondrocytes	Cartilage	3D printed scaffolds were implanted subcutaneously; led to increased cartilage tissue and type-II collagen formation	69

Published on 01 2018. Downloaded on 22.5.2025 22:31:12.

Table 1 *(Contd.)*

Synthetic-biomaterials-based bioinks

Biomaterial	Bioprinting method	Cell type	Target tissue	Cellular response	Ref.
	Pneumatic dispenser	Human chondrocyte cells (C20A4)		Viability of cells on day 1 and day 3 after printing were approximately 90% and 70%	70
PEG	Extrusion-based printing	HUVECs		hMSCs seeded on HUVECs laden printed construct and they spread into empty spaces of that construct at day 4	49
	Extrusion-based printing	NIH-3T3 fibroblasts, HepG2 C3A and Int 407	Vascular	High cell viability up to 4 weeks	110
	Inkjet printing-modified	Bone marrow derived hMSCs (hBMSCs)	Bone	>85% cell viability up to 3 weeks; increased osteogenic marker formation	111
	Extrusion-based printing	hBMSCs		>75% cell viability up to day 7 after printing	112
	Extrusion-based printing	MSCs		Susceptibility of outer cells of the needle edge was higher when shear level was higher than 1639 s^{-1} in poloxamer, a commercially available cream, alginate-based and alginate–gelatin composite bioinks	114
	Extrusion-based printing	NIH-3T3 fibroblasts		More than 50% cells were damaged on the edges of printed GelMA and PEGDA droplets after UV exposure for 5 minutes, however less than 20% cells were damaged on the edges of RAPID bioink after 5 minutes exposure in $CaCl_2$ solution	116
Pluronic	Extrusion-based printing	Primary culture bovine chondrocytes		Cell viability: 62% for pure, 86% for modified Pluronic on day 14	117
HAMA-pHPMA-lac/PEG	Extrusion-based	Primary culture equine chondrocytes	Cartilage	Medium level HAMA concentrations (0.25%–0.5%) promoted cartilage-like matrix production compared to HAMA-free hydrogels; higher (1%) concentrations led to undesirable fibrocartilage formation	118
PG-HA	Extrusion-based	Human and equine MSCs	Articular cartilage	PG-HA bioink showed higher improvement on the cell viability and differentiation with respect to PG-only bioink	119
PVP	Inkjet bioprinting	Neonatal human foreskin fibroblasts (HFF-1)		PVP improved the survival and homogenous dispersion of the printed cells	120

Cell aggregate/pellet-based bioinks

Biomaterial	Bioprinting method	Cell type	Target tissue	Cellular response	Ref.
Cell aggregate/pellet-based bioinks	Extrusion-based printing	CHO		Cellular droplets and sheets were fused after printing	22
	Manual printing	CHO		Minimum number of cells died at the end of each fusion of aggregates	21
	Extrusion-based printing	Chicken cardiomyocytes CHO, human vascular endothelial cells	Cardiac tissue	Synchronous beating was observed after 90 h of bioprinting	127
	Inkjet bioprinting	CHO		No significant difference was found in cell viability between printed and unprinted cells; cell viability of printed cells was 89%	23
	Inkjet bioprinting	D1 murine MSCs, murine mammary cancer cell line (4T07)		Addition of EDTA did not cause significant cell deaths	129
	Extrusion-based printing	MSCs, Schwann cells	Nerve	Extensive axonal re-growth in both the proximal and distal ends of the printed nerve conduits	130
	Extrusion-based printing	Mouse embryonic fibroblast cells	Aorta	No activation of caspase-3 was observed in continuously printed ring cells based bioink	123
	Inkjet bioprinting	Human alveolar epithelial type II cell line A549, hybrid human cell line EA.hy926	Lung	Cell viability was ≥95% for epithelial cells and co-cultures and ≥86% for endothelial cells	105
	Robotic dispensing	Fibroblasts, keratinocytes	Skin	Viability for both cell types was ≥95%; uniform distributions of fibroblasts in the dermal layer and uniform distributions of keratinocytes in the epidermal layer were observed	18
	3D bioprinting with valve-based setup	Human embryonic stem cells, human embryonic kidney cells (HEK293)		Cell viability was more than 95% after 24 h following the printing and more than 89% after 72 h	131

This journal is © The Royal Society of Chemistry 2018

Table 1 *(Contd.)*

Cell aggregate/pellet-based bioinks

Biomaterial	Bioprinting method	Cell type	Target tissue	Cellular response	Ref.
	Dispensing hanging-drops based printing	Adult murine cardiac valve interstitial cells, mouse BMSCs, mouse dermal fibroblasts		Cell aggregates treated with growth factors have higher fusion capacity than the aggregates without growth factor treatment	132
	Extrusion-based printing	CHO, human umbilical vein smooth muscle cells, human skin fibroblasts		Apoptosis was shown with caspase-3 staining of few cells in the printed vascular wall	133
	Custom-made bioprinter with four cartridges	D1 murine MSCs, 4T07		Cells showed higher cell attachment and fidelity of shape of the bioprinted constructs on printing patterns which had units of the smaller areas on collagen covered-coverslips for each cell type	134

Commercial bioinks

Biomaterial	Bioprinting method	Cell type	Target tissue	Cellular response	Ref.
Derma-matrix	Inkjet bioprinting	C2C12 myogenic precursor cells		Histological analysis showed human acellular dermis alone did not result in bone formation and bone formation was limited to the BMP-2-printed half of the constructs	121
Novogel	Extrusion-based printing	Aortic SMCs, human aortic endothelial cells, human dermal fibroblasts, CHO, Schwann cells		After printing, NovoGel was removed and histology results showed vascular structures with cells and cell-produced ECM at 14 days	122
	Extrusion-based printing	HepG2, NIH-3T3 fibroblasts		Cell viability was more than 80% after printing for 8 days	38
	Extrusion-based printing	Mouse embryonic fibroblast cells	Aorta	No activation of caspase-3 in continuously printed bioink ring cells	123

Composite bioinks/bioinks with bioactive molecules

Biomaterial	Bioprinting method	Cell type	Target tissue	Cellular response	Ref.
AuNPs	Extrusion-based printing	NIH-3T3 cells	Vascular	Cells proliferated and secreted ECM up to 4 weeks	86
AgNPs	Extrusion-based printing	Chondrocytes	Cyborg organs/ cartilage	>90% cell viability; high ECM formation up to week 10, cells were alive and metabolically active	135
Magnetic iron oxide particles	Hybrid nano-printing system	Porcine aortic endothelial cells	Vascular	Cell viability decreased with nanoparticles and printing pressure, but did not depend on nozzle diameter	78
Blood plasma	Laser-assisted bioprinting	hASCs	Adipose	Differentiation into adipogenic lineage over 21 days; same amount of proliferation between printed and non-printed samples	148
Cryo bioink	Extrusion-based printing	Red blood cells		Cellular morphology and functionality of the printed patterns were maintained successfully during and after vitrification	149
Ultrashort peptides	Sequential deposition	hMSCs	Vascular/skin	Cell elongation was observed in less than a week; good *in vivo* biocompatibility and stability	12
Genetically engineered phage	Extrusion-based printing	MC3T3-E1	Bone	Higher levels of cell viability, proliferation and differentiation with engineered phages	13
Conductive bioink	Extrusion-based printing	Cardiomyocytes and cardiac fibroblasts	Cardiac tissue	High level expression of cardiomyocyte markers, cell viability 90% and no cytotoxicity of carbon nanotubes on cells during electrical conductivity	137

Published on 01 2018. Downloaded on 22.5.2025 22:31:12.

Published on 01 2018. Downloaded on 22.5.2025 22:31:12.

GelMA constructs. Using a 10% GelMA concentration, good results were obtained with a cell density of 1.5×10^6 cells per mL; however, no significant differences were observed while the UV exposure times were varied from 15 to 60 s UV. Following the characterization, we were able to print various designs of GelMA constructs with good cell viability, proliferation, and spreading. We also demonstrated the bioprinting of 3D GelMA constructs embedded with sacrificial agarose microchannel networks. After removing these sacrificial layers, the perfusion of the constructs with the media was demonstrated, leading to improved mass transport, cellular viability, and the differentiation of osteogenic cells in the GelMA matrix.[38] This method may be beneficial for the vascularization of thick 3D engineered constructs. Kolesky *et al.* recently reported an alternative method by co-printing multiple cell types, ECM-like structures, and embedded vascular structures by a MHDS, where the main bioink matrix was GelMA.[39] To create the vascular network, Pluronic F127 was used as the sacrificial ink, which was then removed after the printing process by liquefying it at a lower temperature (Fig. 2). A MHDS system reduced the printing time needed to create a complex tissue construct and the proposed method had higher survival rates for the multiple cell types encapsulated in GelMA. Other groups have blended GelMA with HA and used this mixture as a hybrid bioink.[27,40,41] In addition to its advantageous properties for creating bone and cartilage tissues, HA can be used to improve the viscosity of GelMA prepolymer solutions. Since the mechanical properties are critical in bioprinting processes, HA can be added to GelMA solutions to create more robust structures, which will be discussed in more detail in the HA section. Both collagen and gelatin are amenable for bioprinting applications; however, to generate tissues with intended mechanical and biochemical properties further characterization is required. As mentioned, the parameter space for printability, cell density, related changes in viscosity, cell viability, *etc*. are quite large and the printing protocols require further experiments and modeling efforts prior to generating tissues with reproducible properties. In case these materials do not possess the proper properties, they will be combined with other materials to create suitable formulations.

During the preparation of bioinks, the relevance of the hydrogels' bioactivity and the related cellular response is an important factor. Daly *et al.* used agarose, alginate, GelMA, and BioINK (methacrylated PEG-based hydrogel) as bioinks for cartilage tissue engineering to analyze the effect of several bioinks on a single cell type.[42] Each hydrogel was blended with MSCs before bioprinting. In addition, polycaprolactone (PCL) microfibers were used to improve the mechanical properties of bioinks during the bioprinting process. In this study, an extrusion-based bioprinting system (3D Bioplotter) was used. It was shown that the alginate and agarose hydrogels supported the formation of hyaline-like cartilage more than the other hydrogels with evidence of higher tissue staining for type II collagen. On the other hand, GelMA and BioINK supported the formation of fibrocartilage-like tissue more than the other groups as proven by the observation of higher amounts of both type I and type II collagen in tissues. Mechanical studies demonstrated that the inclusion of PCL microfibers into bioinks increased the elastic moduli of alginate and GelMA bioinks 544-fold and 45-fold, respectively, and these values were within the range of articular cartilage. Cell viability studies showed that all the bioinks had high levels of MSC viability after bioprinting (~80%). In another study, GelMA hydrogels containing different cell types were bioprinted and the responses of these cells to a single bioink was investigated.[43] Articular cartilage-resident chondroprogenitor cells (ACPCs)-, MSCs-, and chondrocytes-laden GelMA-based hydrogels were used as bioinks for bioprinting. An extrusion-

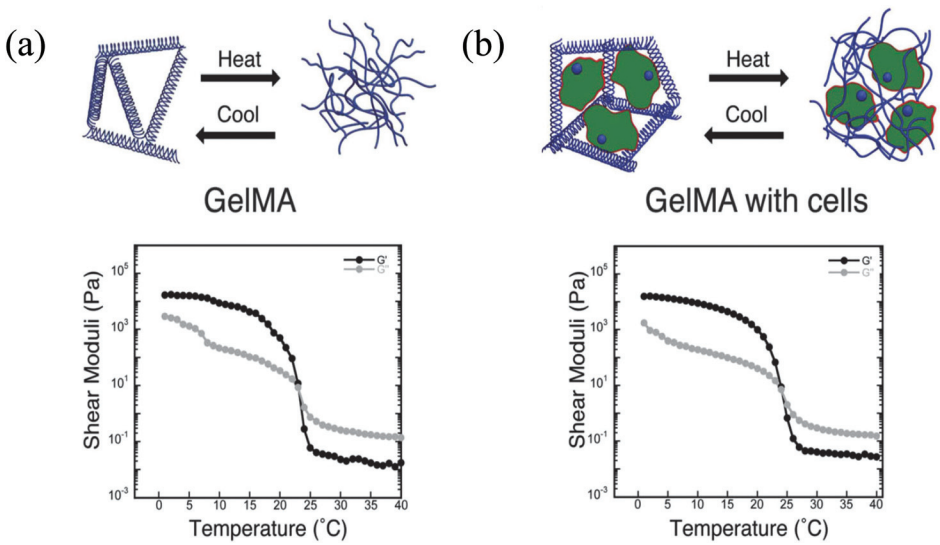

Fig. 2 Schematic diagrams of thermoresponsive gelation and the corresponding shear elastic (G') and loss moduli (G'') measured as a function of temperature for: (a) pure GelMA, and (b) fibroblast-laden GelMA bioinks.[39] Reprinted with permission Copyright John Wiley & Sons, Inc., 2014.

 This journal is © The Royal Society of Chemistry 2018

Published on 01 2018. Downloaded on 22.5.2025 22:31:12.

based bioprinter with BioCAD software was used. The results showed that the ACPCs had better behavior than the chondrocytes regarding the production of neo-cartilage. In addition, unlike MSCs, ACPCs demonstrated the lowest gene expression of hypertrophy marker collagen type X and the highest expression of PRG4, which encodes an important protein (lubricin) in joint lubrication. ACPC- and MSC-laden bioinks were combined in a multi-compartment structure to prepare a bioprinted model of articular cartilage, which showed apparent deep and superficial zones with distinct ECM compositions. Furthermore, it was shown that different cell types demonstrated different cell responses to the same bioink.

Fibrinogen is a large, fibrous, and soluble glycoprotein that is involved in blood clot formation, where it is converted into an insoluble fibrin molecule by thrombin in the presence of Ca^{2+} *via* intermolecular interactions.[44,45] In tissue engineering, fibrinogen and fibrin are mainly used to fabricate functional tissue constructs for the replacement of damaged tissues due to their beneficial roles in wound healing. They are biocompatible, biodegradable, and non-immunogenic, and induce cell attachment, proliferation, and ECM formation.[44,45]

Nakamura *et al.* created bioinks using fibrin and alginate and used them to bioprint structures using a custom-made inkjet bioprinter.[46] In this bioink formulation, fibrin had a better cellular response, while alginate was a better material to use to enable seamless bioprinting. Other composite bioink forms are also available, such as fibrin-collagen, which was combined with inkjet printing and electrospinning to improve the mechanical properties of the final construct for cartilage tissue engineering.[47] The constructs were fabricated in three steps: first, PCL was electrospun as a substrate, then chondrocytes were encapsulated in fibrin/collagen and bioprinted on top of the PCL layer, and finally another PCL layer was deposited using electrospinning. They found that this hybrid system improved the mechanical properties of the construct and did not affect the cell survival rates. This new system may be utilized for the formation of complex tissues. Gruene *et al.* used fibrinogen as a bioink by mixing it with HA and used the LaBP method for the 3D assembly of multicellular arrays.[48] ASCs or endothelial colony-forming cells (ECFCs) were encapsulated in a fibrinogen–HA mixture and then individual cell types were separately bioprinted in a layer-by-layer fashion. The bioprinting surface was covered with fibrin as a biopaper and thrombin was sprayed on it to enable gelation and fixation of the bioprinted HA/fibrinogen droplets. They demonstrated the formation of a vascular-like network, which indicated the presence of interactions between the printed ASCs and ECFCs from different layers. Alternatively, Rutz *et al.* blended fibrinogen with PEG or a PEG–gelatin mixture.[49] They found that the incorporation of fibrinogen significantly increased the degradation time and improved the robustness of the constructs after cross-linking with thrombin/Ca^{2+} solution following the bioprinting. Fibrinogen was also used as a biopaper for printing cell spheroids to fabricate microvasculature networks.[45]

Silk is a natural polymer that has been used for centuries as a suture material in medical applications. It has numerous attractive properties as a biomaterial since it is highly elastic and has a slow degradation rate that is needed for providing sufficient support for the cells until the new tissue is regenerated. In addition, it has a low immunogenicity and is biocompatible, hence it is also suitable for clinical applications.[50] Due to these attractive properties, silk has long been utilized as a scaffolding material for both soft and hard tissue engineering applications. Recently, it has also been adapted for bioprinting applications. Schacht *et al.* investigated the use of recombinant spider silk to create hydrogels.[51] In this study, mouse fibroblasts were either cultured on bioprinted spider silk-based hydrogels or were encapsulated inside the bioink material. It was found that the viability of the encapsulated cells and the bioprinted cells were lower than the cells simply seeded without using a bioprinter. Alternatively, a bioink was prepared by including human nasal inferior turbinate-derived mesenchymal progenitor cells into a mixture of gelatin and silk fibroin (Fig. 3).[52] It was found that the prepared hydrogels, which were enzymatically cross-linked using a mushroom tyrosinase-supported chondrogenic and adipogenic differentiations. In contrast, the hydrogels cross-linked using sonication supported osteogenic differentiation. The variations in cellular response were due to the use of different cross-linking methods during bioprinting. The enzyme mushroom tyrosinase oxidized the tyrosine residues of gelatin/silk into reactive elements that could react with each other or available amines, while sonication changed the hydrophobicity and increased the silk fibroin self-assembly to enable physical cross-linking.

2.2. Polysaccharides

Alginate, also known as alginic acid, is a natural anionic polysaccharide refined from brown seaweed and is similar to the glycosaminoglycans found in the native ECM of the human body. It has been commonly used in biomedicine due to its biocompatibility, low cytotoxicity, mild gelation process, and low cost.[53,54] In particular, it has been widely used as a bioink because of its fast gelation property under physiological conditions without forming harmful byproducts.[55,56] The gelation of alginate can be easily induced in the presence of divalent cations such as Ca^{2+} and Ba^{2+} by forming bridges between polymer chains, enabling physical cross-linking and solidification.[57,58] The removal of the ionically cross-linked alginate gels from a construct can occur *via* dissolution by release of the divalent ions cross-linking the hydrogel by exchange reactions with monovalent cations present in the surrounding medium.[53]

Since fast gelation leads to good printability, most of the current bioprinting methods have utilized alginate or modified alginate alone, or alginate blended with other biomaterials as bioinks. For example, Yu *et al.* developed a method to bioprint vascular-like channels by encapsulating cartilage progenitor cells in alginate and obtained cell-laden hollow tubular constructs with good mechanical and biological properties.[59] They

Published on 01 2018. Downloaded on 22.5.2025 22:31:12.

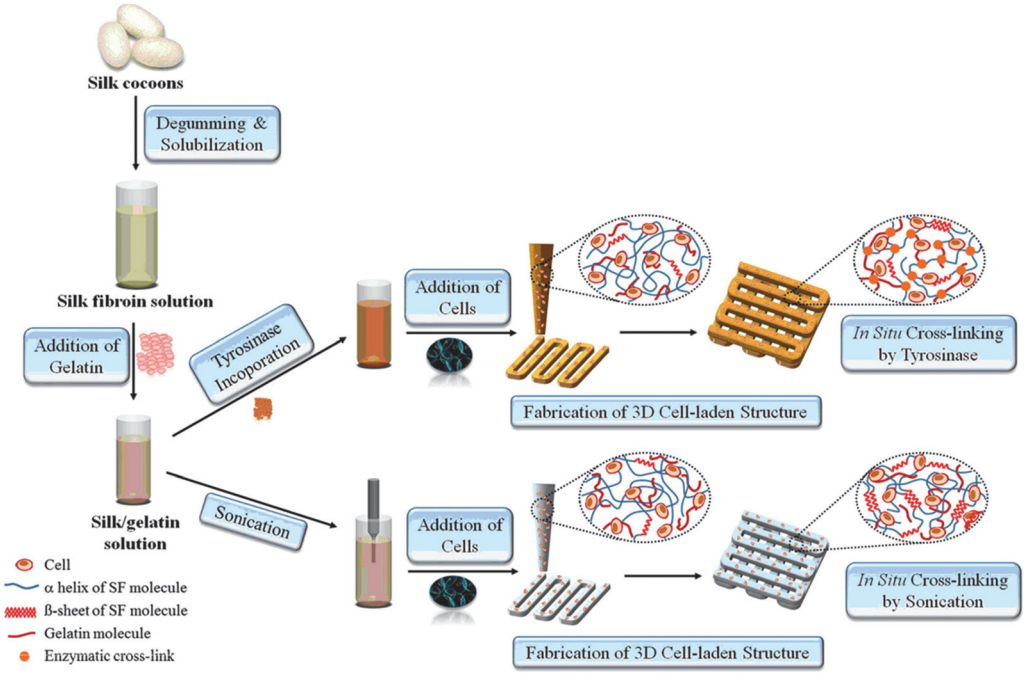

Fig. 3 The process of 3D-bioprinting of cell-encapsulated constructs by using silk-gelatin as a bioink.[52] Reprinted with permission Copyright Elsevier, 2014.

designed a coaxial nozzle system, whereby an alginate solution was extruded through the sheath and a $CaCl_2$ solution was delivered in the core forming a tubular structure. This system combined a single-nozzle bioprinter and a motion unit to enable extrusion-based bioprinting. It was noted that increasing the alginate concentration from 2% to 6% (w/v) significantly reduced the cell viability due to the increase in shear stress during extrusion resulting from the increased viscosity. The same group further investigated the parameters that affected the diameter of the bioprinted filaments and the gene expression profiles of the encapsulated cells using the same printing procedure.[60] Higher cell-specific gene expressions were observed, thus confirming the functionality and higher differentiation ability of the cells within the bioprinted perfusable alginate tubes compared to monolayer cultured cells. Recently, they also encapsulated human umbilical vein SMCs in alginate and, while using the same printing method, they investigated the dehydration, swelling, and degradation characteristics of the constructs in addition to ECM deposition of cells.[54] In general, higher alginate concentrations were found to result in a lower cell viability, degradation rate, porosity, and permeability, with 4% (w/v) alginate suggested as the optimum concentration for the bioprinting process, where ECM formation was observed on both surfaces of the bioprinted tubes. Similarly, Gao *et al.* used the same coaxial system for bioprinting an alginate bioink to fabricate hollow tubes.[61] They gradually immersed the stage into a $CaCl_2$ solution to further cross-link the construct, a promising process with applications for achieving large-scale tissue bioprinting (Fig. 4).

Alginate was also widely used as a bioink in the LaBP method, which is a promising technique for scaled-up bioprinting with cellular resolution. In a typical process, a quartz disk with a thin layer of cell-alginate coating is used. A laser is focused on top of the quartz disk featuring an optically absorbing layer, which generates local heating and creates a vapor bubble in the underlying cell-alginate coating. The bubble then expands and forces the formation of a droplet, which is ejected into a $CaCl_2$ bath (Fig. 5).[62] In LaBP, the gelation parameters and the concentration of alginate affect the cellular viability. It was found that 2 min gelation led to higher cell viability than 10 min gelation, which implied that a thin bioink membrane was needed, whereas a thicker one could, on the contrary, block the transport of oxygen and nutrients.[62] In a subsequent study, they further tested different alginate concentrations from 1–3% (w/v), and found that higher alginate concentrations resulted in lower viability, due to transport limitations. Another group using a similar LaBP method studied the effect of the viscosity of the bioinks using different laser printing parameters.[63] By using higher alginate concentrations with higher viscosities, they were able to obtain droplets with smaller diameters that enabled them to increase the resolution of the printed structures. Therefore, there seems to be a balance in cell viability and resolution, thus necessitating precise tuning of the alginate concentration as a bioink to meet the needs of different applications. Increasing the concentration of encapsulated cells further increased the viscosity and allowed them to bioprint constructs with higher cell densities *de novo*. LaBP was also used for developing a single-step fabrication of cell-encapsulated alginate microbeads with

 This journal is © The Royal Society of Chemistry 2018

Published on 01 2018. Downloaded on 22.5.2025 22:31:12.

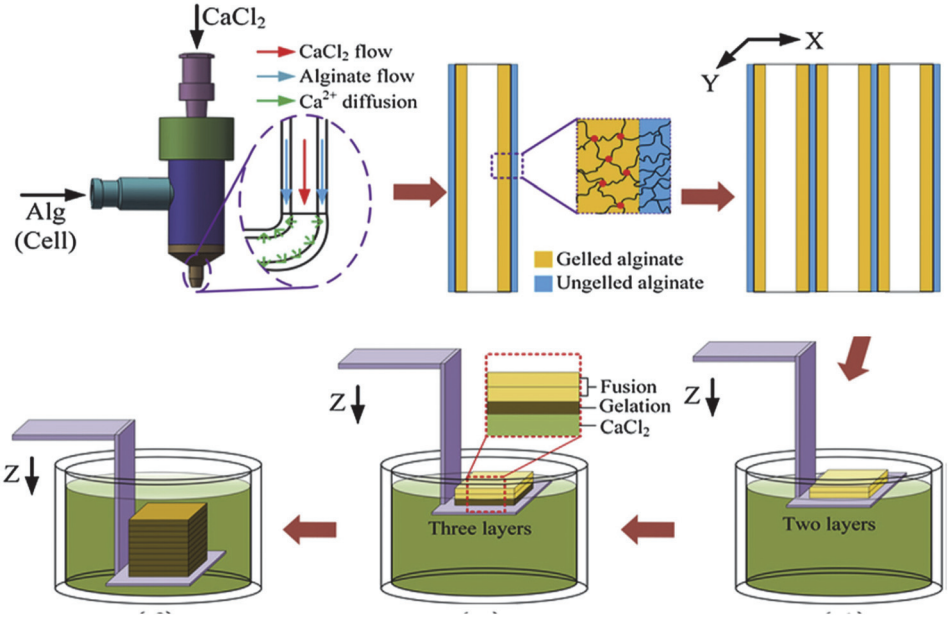

Fig. 4 Bioprinting process of a 3D structure with built-in microchannels by using an alginate bioink. Physical cross-linking process was utilized *via* calcium ions.[61] Reprinted with permission Copyright Elsevier, 2015.

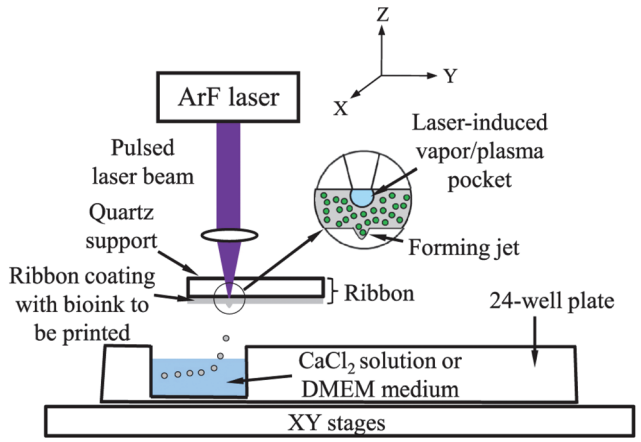

Fig. 5 Schematic representation of laser-assisted bioprinting.[62] Reprinted with permission Copyright IOP Publishing, 2014.

precise pattern definition and delivery.[64] The laser was programmed to provide a single pulse to deposit each corresponding target spot and to eject a mixture of cancer cells and alginate onto a gelatin-$CaCl_2$-coated substrate, where the bioprinted droplets were cross-linked with $CaCl_2$ *in situ* to form microbeads. A higher cell viability and a better resolution were achieved with this system. Similarly, Gasperini *et al.* bioprinted cell-containing alginate beads onto the same gelatin-$CaCl_2$ coating by using an electrohydrodynamic deposition process.[65] In this approach, the tip of the bioprinter nozzle was connected to an electrical pulse generator with high voltage, which was used to overcome the problems associated with surface tension occurring at the tip of the liquid dispenser. The technique was compatible with the fabrication of 3D tissue constructs *via* the deposition of single dots or continuous lines and enabled precise positioning with high cell viability. In another study, Williams *et al.* utilized alginate for bioprinting spheroids fabricated from ASCs by using a droplet-based bioprinting method.[66] The main component of their bioprinting system was a pen-like device, which was precisely controlled and the liquid delivery unit enabled them to create spheroids reproducibly with minimal variations in size. They found that the encapsulated cells were uniformly dispersed in the alginate construct and maintained good cell viability. This system provided a platform that allowed control over the quantity of cells in each spheroid, which is an important feature for controlled cell delivery in regenerative medicine.

Khalil *et al.* encapsulated endothelial cells inside alginate and characterized the porous cell-laden alginate constructs created after a direct cell writing process by using an inkjet-based method and MHDS.[9] They obtained high cell viability after bioprinting and found that 1.5% (w/v) alginate and 0.5% (w/v) $CaCl_2$ were the optimum concentrations in their process. They reported a 1/3 decrease in the mechanical strength of the constructs by the end of 3 weeks. The same group also investigated the relationship between the shear stress that the cells experience during dispensing and cellular viability.[67] They encapsulated endothelial cells inside the bioink and found that the survival rates of the cells decreased by around 40% when the bioprinting pressure was increased from 5 psi to 40 psi. Furthermore, bioprinting processes utilizing a nozzle with a smaller-diameter were also found to decrease the viability of cells, but with a less pronounced effect. Using the same method, Chang *et al.* utilized alginate as a bioink and engineered a microchip model for the drug metabolism studies of

Published on 01 2018. Downloaded on 22.5.2025 22:31:12.

liver tissue organoids.[68] In this work, using MHDS, they carried out a layer-by-layer deposition of cells and other biological materials simultaneously and then integrated the 3D-bioprinted construct with a microfluidic system. Alginate bioinks with concentrations ranging from 1.5–3% (w/v) were used for encapsulating hepatocytes, but no significant difference was found in drug metabolism studies when different alginate concentrations were used. They also compared a static culture with a perfusion culture and observed significantly increased metabolism levels for the perfused system. Alginate was mixed with a synthetic polymer PCL to create a hybrid material with enhanced mechanical properties and was then bioprinted using inkjet bioprinting. In this study, a MHDS was first used to print the PCL frame, where the gaps in that frame were subsequently filled by bioprinting alginate laden with cells and growth factors. It was shown that this hybrid bioink system supported cartilage regeneration both *in vitro* and *in vivo*.[69] Schuurman *et al.* successfully used the same approach for bioprinting and demonstrated the encapsulation of chondrocytes with an alginate–PCL hybrid material.[70]

A bioink made of alginate containing fibroblasts could also be used to fabricate complex patterns of tubes using inkjet bioprinting.[71] The group used drop-on-demand inkjet printing and vertically bioprinted cell-laden zigzag tubes with high post-printing cell viability and also found that the maximum height of the bioprinted tubes could be determined by the inclination angle of the construct. Using the same bioprinting setup, the group investigated the effect of cell concentrations on droplet formation and on the bioprinting process.[72] In addition, they compared the effect of soft particles (cells) and hard particles (polystyrene microbeads) on droplet formation and on the properties of the bioprinted structures. It was found that factors such as increasing the cell concentrations and using cells instead of microbeads decreased the diameter of the droplets, reduced the dispensing velocity, and increased the breakup time. Mobed-Miremadi *et al.* used alginate as a bioink to encapsulate bacteria to obtain miniature spherical microbeads using inkjet bioprinting.[73] They reported rheological characterization and optimum operating conditions to create miniaturized beads utilizing bioprinting.

In summary, due to its capability for fast physical gelation and broadly tunable viscosity, alginate has become the most widely used natural polymer for bioprinting and is probably the most common material of choice in proof-of-concept studies for *in vivo* applications. However, alginate is a relatively biologically inert material as indicated by the fact that it does not possess cell-adhesive moieties, consequently leading to limited cell attachment. To address this issue for bioprinting applications, Jia *et al.* chemically modified alginate by an oxidation process.[55] After the oxidation step, they conjugated RGD peptides onto alginate to allow bioactivity and promote cell binding sites. They studied different concentrations and oxidation rates and found that these modified alginate-based bioinks supported the growth and spreading of human ASCs after bioprinting. The tunability of these bioinks could be useful in meeting tissue-specific requirements for different 3D bioprinting applications. Furthermore, it is common to use composite materials to fulfill the physicochemical requirements of different tissues and organs. While alginate alone or its modified forms can be used as bioinks for different bioprinting applications, alginate has also been combined with other biomaterials to create composite bioink formulations. Some of these materials include HA, fibrin, thrombin, collagen, gelatin, agarose, Matrigel, genetically engineered phage, as well as nanoparticles such as HAp and magnetic iron oxide particles, which are discussed in other sections of this review where applicable.

Gellan gum is a hydrophilic and high-molecular weight anionic polysaccharide produced by bacteria. Similar to alginate, it forms a hydrogel at low temperatures when blended with monovalent or divalent cations.[74] It has been approved by the United States Food and Drug Administration (FDA) as a direct food additive[75] and is widely used in the food and pharmaceutical industries as a gelling agent and stabilizer as well as in regenerative medicine applications as a viable substrate for the engineering of tissues. From a bioprinting perspective, gellan gum has been combined with other polymers to prepare bioinks with attractive rheological properties and to improve the shape fidelity of the bioprinted constructs.[76,77] The viscosity controls the resolution of the printed structures and drastically affects the printing of pre-defined 3D constructs.[78] Moreover, gellan gum is relatively inexpensive to produce, and has fine processability and tunable mechanical properties that are important for bioprinting processes.[79]

Melchels *et al.* combined low-concentration gellan gum with GelMA as the bioink, utilizing the favorable bioactive properties of GelMA and the overall improved printability and cell response of the composite.[77] This composite bioink was mixed with a salt solution to induce the formation of a gel-like structure by the ionic network formed between the gellan gum chains and the interactions between the negatively charged gellan gum residues and the positively charged GelMA residues. The second cross-linking step was done by decreasing the temperature, which enabled the physical cross-linking of GelMA. Finally, to fix the bioprinted construct, GelMA was further chemically cross-linked utilizing UV. The results concluded that the addition of the gellan gum improved the viscosity and hence the printability of the bioink and did not affect the microstructure of the construct or the survival of osteoblastic cells. In another similar study, gellan gum was mixed with GelMA to prepare a bioink and the mixture was used for the encapsulation of chondrocytes. Additionally, sacrificial layers consisting of poly(vinyl alcohol) (PVA), PCL, and alginate were used to support the bioprinted construct. These sacrificial layers were deposited at the same time with the bioink and were then removed after bioprinting by immersing in aqueous solutions. Cell-laden constructs with clinically relevant dimensions were successfully fabricated by this multi-step printing approach.[80] The same group combined a gellan gum–GelMA bioink mixture with MSC-laden polylactide microcarriers.[81] The microcarriers improved the mechanical strength of the hydrogel mixture, while the bioprinted bilayer

 This journal is © The Royal Society of Chemistry 2018

Published on 01 2018. Downloaded on 22.5.2025 22:31:12.

cylindrical grafts supported cell viability, spreading, and osteogenic differentiation. The overall results suggested that the gellan gum had no negative effect on cell growth and differentiation and was safe to use as a supportive bioink. In a recent study, gellan gum was combined with RGD peptide, and the mixture was used as a novel hybrid bioink, whereby primary neural cells were encapsulated in this bioink for the 3D bioprinting of constructs to obtain brain-like structures with discrete layers.[79] An extrusion-based hand-held bioprinting technique was used to obtain multilayer cortical structures. This hand-held method was developed for practical use in cell culture studies without the need for a sophisticated bioprinting device. They observed that the incorporation of RGD sites into the gellan gum induced cell growth and network formation compared with the results obtained from gellan gum alone. Therefore, this bioink seemed promising for creating biomimetic 3D structures.

HA is a non-sulfated glycosaminoglycan found in the natural ECM. It plays a substantial role in synovial fluid, vitreous humor, and hyaline cartilage.[82] When dissolved in water, HA solution has a viscous property, making it a promising material for applications in tissue engineering.[83] In addition to its advantageous properties in engineering bone and cartilage tissue constructs, HA provides a means to produce solutions with low viscosity since it was reported that when the shear rate increases, there is a need for a longer relaxation time for HA molecules to reorient, thus causing the loss of viscosity.[84] It is also suitable for bioprinting applications where good rheological properties and high viscosity are required as it was noted that when the concentration and molecular weight of HA are higher, the viscosity of HA solutions are found to increase.[84] In a recent study, to create an osteochondral interface, two rectangular sections were printed with PCL as the support. One part was filled by bioprinting chondrocytes/osteoblasts encapsulated in an HA hydrogel mixed with alginate, while the other part was encapsulated with collagen type I.[85] The viability of the encapsulated cells was next evaluated. The results demonstrated that the osteoblasts encapsulated in collagen I hydrogel had more than 90% viability and showed a higher expression of osteogenic markers (Runt-related transcription factor 2 [RUNX2] and alkaline phosphatase [ALP]) than osteoblasts encapsulated in the HA-based hydrogel. On the other hand, chondrocytes cultured on the HA-based hydrogels showed higher expression levels of chondrogenic markers (collagen II and aggrecan) than those cultured in collagen I hydrogel, implying that different cell lineages require different bioink formulations to function properly. Methacrylated HA (HAMA), a photocross-linkable form of HA, was utilized to prepare trileaflet valve constructs.[41] In this study, a 3D bioprinter with a dual syringe system was used to obtain bioprinted heart valves. The root of a heart valve was printed by using a hydrogel without cells, and subsequently leaflets of the valves were printed with HAMA-GelMA hydrogels containing human aortic valvular interstitial cells. It was reported that the bioprinted heart valves had high cell viability (>90%), aided by the deposition of an ECM matrix consisting of collagen and glyosaminoglycans. In another study, a methacrylated ethanolamide derivative of gelatin (GeMA) and HAMA were used with human hepatocellular carcinoma cells, human intestinal epithelial cells, and murine fibroblasts as the bioink for bioprinting.[40] *In vitro* cell biocompatibility results showed that a mixture of GeMA and HAMA hydrogels supported the attachment and proliferation of the cells. In this study, cell-free scaffolds or human hepatocellular carcinoma cells-loaded hydrogels were bioprinted and tubular constructs were formed by using an extrusion-based system, with UV irradiation applied to chemically cross-link GeMA and HAMA. It was observed that the cells attached only to the parts of the hydrogel that contained GeMA and HAMA together but did not attach to the parts consisting of HAMA alone. The same group studied gold nanoparticles (AuNPs) and thiol-modified polymers derived from HA and gelatin as printable semi-synthetic ECM (sECM) hydrogels. The AuNPs here were used as active multivalent cross-linkers for thiol-modified HA and gelatin. In the bioprinting process, cell-containing and cell-free bioinks were used to make tubular structures with a polymer solution of AuNPs-thiol-modified HA and thiol-modified gelatin in a vertical ring shape.[86] Human hepatocellular carcinoma cells, human intestinal epithelial cells, and murine fibroblasts were cultured on AuNPs-sECM hydrogels, and the viability results showed ≥95% cell viability at both day 3 and day 7. During and after bioprinting, the cell-laden sECM hydrogels maintained their shapes. GelMA and GelMA-HA hydrogels were also used with a BioScaffolder dispensing system to create chondrogenic structures.[27] The physical properties of the GelMA hydrogels were modified by changing the UV exposure time, the concentration of the hydrogels, and the incorporation of mechanically supportive polymers, such as PCL. After 3 days, the viability of the chondrocytes seeded on bioprinted GelMA and GelMA-HA scaffolds were found to be around 73% and 82%, respectively. Kesti *et al.* used a glycosaminoglycan-based hydrogel system by mixing poly(*N*-isopropylacrylamide)-grafted HA (HA-pNIPAAM) with HAMA to obtain a versatile structure with a thermoresponsive polymer and a photocross-linkable polymer in the hydrogel mixture (Fig. 6).[87] A BioFactory bioprinter, which is a MHDS, was equipped with temperature control and a UV-light source and was used to bioprint bioink layers consisting of bovine chondrocytes encapsulated in the hydrogel. Cell viability studies revealed that embedding the cells in the bioink caused cell death, while after removal of the HA-pNIPAAM, they observed high cell viability, most probably because of the formation of pores and improved diffusion.

Dextran is another natural polysaccharide that has been widely used in tissue engineering applications, since it is non-toxic and hydrophilic. Dextran can be degraded in mammalian tissues by dextranase, hence it is classified as a biodegradable material.[88] Pescosolido *et al.* utilized HA and methacrylated dextran (dexHEMA) to prepare hydrogels that possessed a polysaccharidic semi-interpenetrating polymer network.[89] In this study, a pneumatic dispensing system with a motorized stage was used and equine chondrocytes were encapsulated inside the bioink. The results showed that the HA-dexHEMA mixtures

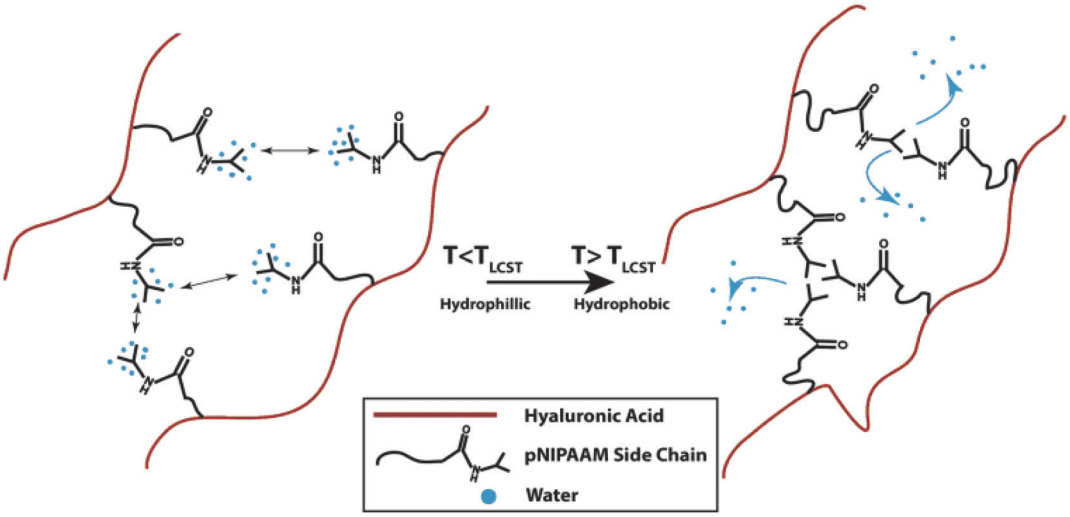

Fig. 6 The gelation process of HA grafted with pNIPAAM.[87] Reprinted with permission Copyright Elsevier, 2014.

Published on 01 2018. Downloaded on 22.5.2025 22:31:12.

had attractive viscoelastic and pseudoplastic features as a bioink and may be used in various bioprinting applications.

Agarose is a polysaccharide extracted from marine algae and seaweed. It is widely used in molecular biology especially for electrophoresis applications as well as in tissue engineering because of its gelling property.[90] In a recent bioprinting study, primary bladder SMCs were embedded inside a collagen gel and then the mixture was printed as droplets.[19] To prepare a collagen-coated structure, an empty Petri dish was first coated with agarose and then with a layer of collagen. Cell-containing collagen droplets were bioprinted on a collagen layer. The results indicated high cell viabilities of approximately 95%. In addition, it was observed that the cells inside the bioprinted constructs started to express transmembrane protein connexin-43, which has important functions in intercellular communication. Neufurth *et al.* used a mixture of alginate–gelatin–SaOS2 cells as the bioink for 3D bioprinting.[30] After bioprinting, the cells were supplemented with polyP.Ca^{2+} and with/without osteogenic cocktail. The inclusion of polyP.Ca^{2+} significantly increased cell proliferation. In another study, agarose with a low melting point and alginate with low viscosity were utilized to prepare a bioink.[91] Human osteosarcoma cells were used for cell patterning studies and the cells were mixed with melted agarose gels and then kept at 36 °C for bioprinting. Mouse fibroblasts were mixed with alginate for extrusion-based bioprinting. The bioprinted constructs were submerged in a high-density fluorocarbon liquid to support their shape. Individual drops of the cell-laden hydrogels were bioprinted layer-by-layer to prepare a 3D tissue construct. Cell viability results showed that the viability after 1, 4, and 7 days following bioprinting were 96%, 99%, and 97%, respectively. Human MSCs with an osteosarcoma origin were also encapsulated in an agarose hydrogel.[92] Next, the prepared bioink was submerged and bioprinted inside a hydrophobic perfluorotributylamine fluid with a high density, where the process supported the bioprinted construct mechanically (Fig. 7). The

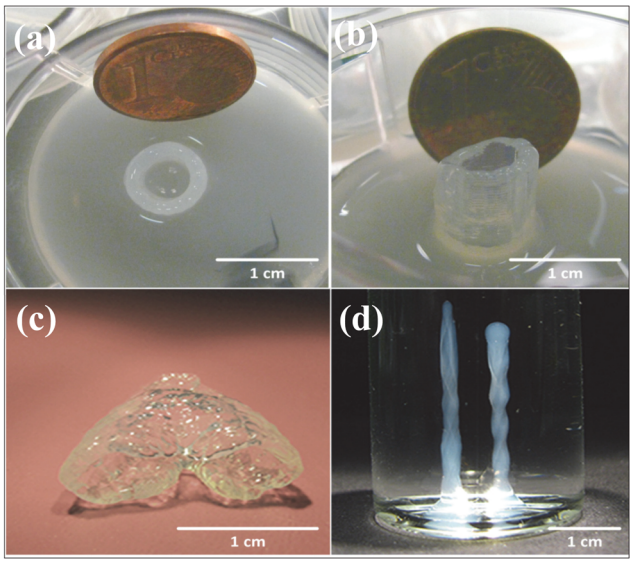

Fig. 7 Robotic and manual printing of 3D constructs by using an agarose bioink under fluorocarbon. (a) Top and (b) side view of printed cell-laden constructs. (c) 3D construct mimicking a vascular bifurcation that was printed while submerged in perfluorotributylamine. (d) Printed cylinders without cells.[92] Reprinted with permission Copyright IOP Publishing, 2013.

results showed that the cells were viable 24 h after bioprinting and after 21 days in culture. Xu *et al.* further investigated *E. coli* as a porogen factor in an agarose hydrogel.[93] To generate microfluidic channels, the *E. coli*–agarose mixture was bioprinted onto a Petri dish pre-coated with a layer of agarose. Next, the hydrogel structure was treated with sodium dodecyl sulfate and the *E. coli* debris was then removed. Murine embryonic fibroblasts were seeded on porous agarose scaffolds and their viability was evaluated. Fibroblasts cultured on 1% agarose gels became confluent after 6 days, while the ones cul-

 This journal is © The Royal Society of Chemistry 2018

Published on 01 2018. Downloaded on 22.5.2025 22:31:12.

tured on 2% agarose gels became confluent after 14 days. Their results demonstrated that the cells stayed alive for 2 weeks on these scaffolds.

Chitosan is another biocompatible and biodegradable polysaccharide with anti-bacterial and wound healing properties.[94] Chitosan can be obtained by the partial deacetylation of chitin and can also be used as a gel-forming material. Due to these properties, it is a promising biomaterial for tissue engineering applications.[95,96] Duarte Campos *et al.* studied the effects of bioprinted collagen, agarose, collagen–agarose, and chitosan–agarose hydrogels on human MSCs and the differentiation of cells into osteogenic or adipogenic lineage.[20] After 21 days of incubation, live/dead staining showed that the cell viabilities were more than 95% for all the groups. The results demonstrated that in a stiff collagen matrix, the cells tended to differentiate into the osteogenic lineage, while in a soft agarose matrix, the cells mostly differentiated into adipogenic tissues.

2.3. dECM-based bioinks

Decellularization is a process used to remove the cellular components of tissues and organs by using chemical agents as well as by physical and mechanical processes.[97] To perform decellularization, many agents have been proposed in the literature, including for instance, non-ionic, ionic, and zwitterionic detergents as well as enzymatic and physical agents.[97,98] For novel bioink formulations that are tissue-specific, Pati *et al.* developed dECM-based bioinks to mimic specific natural environments of various tissue types.[99] They successfully obtained high cell survival rates and cell line-specific gene expression and ECM formation with bioprinted decellularized adipose, heart, and cartilage tissue structures. The bioprinting process for dECM bioinks is shown in Fig. 8. The same group prepared a decellularized adipose tissue matrix by using sodium dodecyl sulfate, where the decellularized matrix was used to encapsulate the ASCs (Fig. 9).[100] DNA quantification showed that most of the DNA content was removed after decellularization with less than 3% DNA content remaining. A bioprinting system with six printheads was used to extrude dECM and PCL at the same time, where PCL was used as a framework to print the cell-laden decellularized adipose tissue matrix. In another study, Skardal *et al.* used Triton X-100 to obtain dECM from skeletal muscle, liver, and cardiac tissues. dECM was mixed with the hydrogel solution and transferred into the cartridge of the bioprinter.[101] In the hydrogel bioink solution, 4-arm and 8-arm PEG or PEG diacrylate (PEGDA) was used with thiolated HA or thiolated gelatin to provide for cross-linking reactions between the acrylate and thiol groups during the first cross-linking step (Fig. 10). After the first cross-linking step, UV was applied to induce secondary cross-linking to form a stable hydrogel structure. To analyze the functionality of the bioprinted liver constructs, primary human liver spheroids were used in the hydrogel prepolymer solution, where the printed tissue construct produced detectable levels of albumin and urea.

Matrigel is a reconstituted basement membrane extracted from the mouse sarcoma ECM and includes essential bioactive

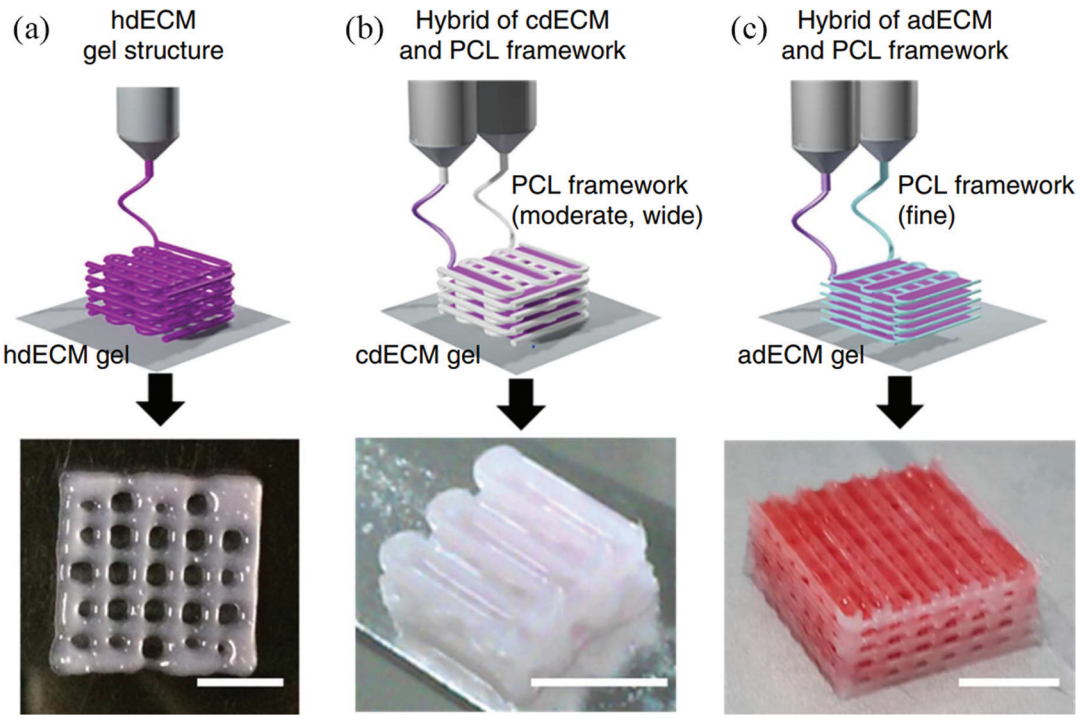

Fig. 8 Utilizing various dECM bioinks for bioprinting 3D tissue constructs. (a) Heart tissue construct was printed with only heart dECM (hdECM). (b) Cartilage and adipose tissues were printed with cartilage dECM (cdECM) and (c) adipose dECM (adECM), respectively, and in combination with PCL framework (scale bar, 5 mm).[99] Reprinted with permission Copyright Nature Publishing Group, 2014.

Published on 01 2018. Downloaded on 22.5.2025 22:31:12.

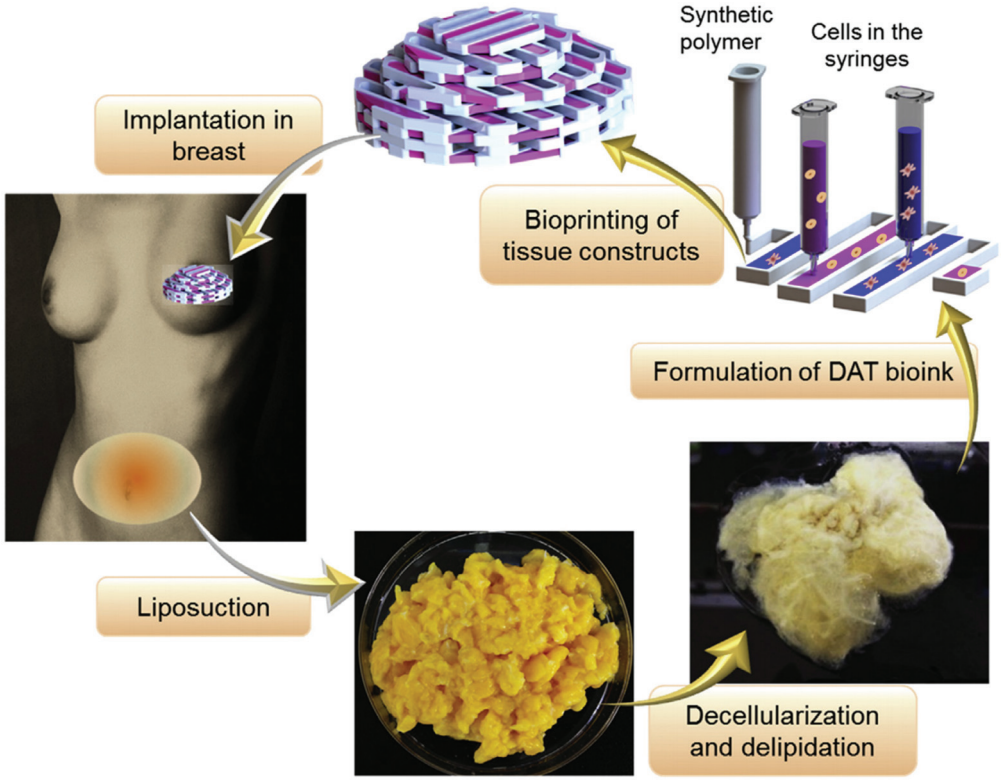

Fig. 9 Adipose tissue obtained by surgery and used as a bioink after a decellularization process for soft tissue reconstruction.[100] Reprinted with permission Copyright Elsevier, 2015.

molecules, such as laminin, collagen, and a set of growth factors.[102,103] It serves as a natural biomimetic ECM and is widely used in cell and tissue cultures, where it undergoes thermal cross-linking at higher temperatures.[104,105] Poldervaart *et al.* used Matrigel in combination with alginate as a bioink for vascularization studies.[106] Similar to other studies, alginate was added to improve the printability of Matrigel. They also incorporated vascular endothelial growth factor (VEGF) into the bioink either directly or within microspheres, which enabled its controlled release. They used a bioprinter with a pneumatic dispensing system for the bioprinting of human EPC-laden hybrid constructs. The results revealed that, although the addition of alginate improved bioprinting, the degradation rates increased and the rate of formation of vessel-like structures decreased, implying that the types of materials and their ratios are critical parameters to adjust when developing an optimum bioink. Matrigel has also been used for bioprinting a drug discovery platform as part of a microfluidic system.[103] Here, the research group used an extrusion-based system for bioprinting hepatocyte-laden or epithelial cell-laden bioinks and designed a temperature controller to prevent thermal gelation of the Matrigel before bioprinting. With this novel system, they successfully fabricated functional dual tissue constructs (hepatocyte and epithelial tissue) and evaluated their synergistic effect under radiation tests for space applications. In other applications, Matrigel was used as a biopaper for coating the surfaces to support bioprinted cells[63,104] or for bioprinting it to the surface without cells for post-printing cell seeding.[105] However, the major issue associated with Matrigel is that it is obtained from murine sarcoma cells and hence its suitability for clinical translation may be limited.[12]

2.4. Synthetic polymer-based bioinks

PEG is a synthetic polymer synthesized by ethylene oxide polymerization, which can be prepared with different chain lengths as well as different structures, such as linear or multi-armed structures. It is a favorable synthetic material because of its tailorable but typically strong mechanical properties that facilitate the bioprinting processes and shape maintenance of the deposited constructs. Non-cytotoxicity (at higher molecular weights) and non-immunogenicity are the other advantages of PEG. On the other hand, it is a bioinert material that the cells cannot readily attach to,[107,108] and therefore it needs to be combined with other biologically active hydrogels. Indeed, composites of PEG and natural biomaterials have been shown to improve the degradation properties of PEG-based constructs.[36,49] In addition, even though PEG is generally accepted to be non-immunogenic, there are several clinical studies where PEG-specific antibodies have been found in patients treated with PEGylated therapeutic enzymes.[109]

Rutz *et al.* utilized PEG to develop tunable bioink formulations with a wide range of mechanical and rheological properties.[49] They produced PEG with reactive groups (PEGX), and

 This journal is © The Royal Society of Chemistry 2018

Published on 01 2018. Downloaded on 22.5.2025 22:31:12.

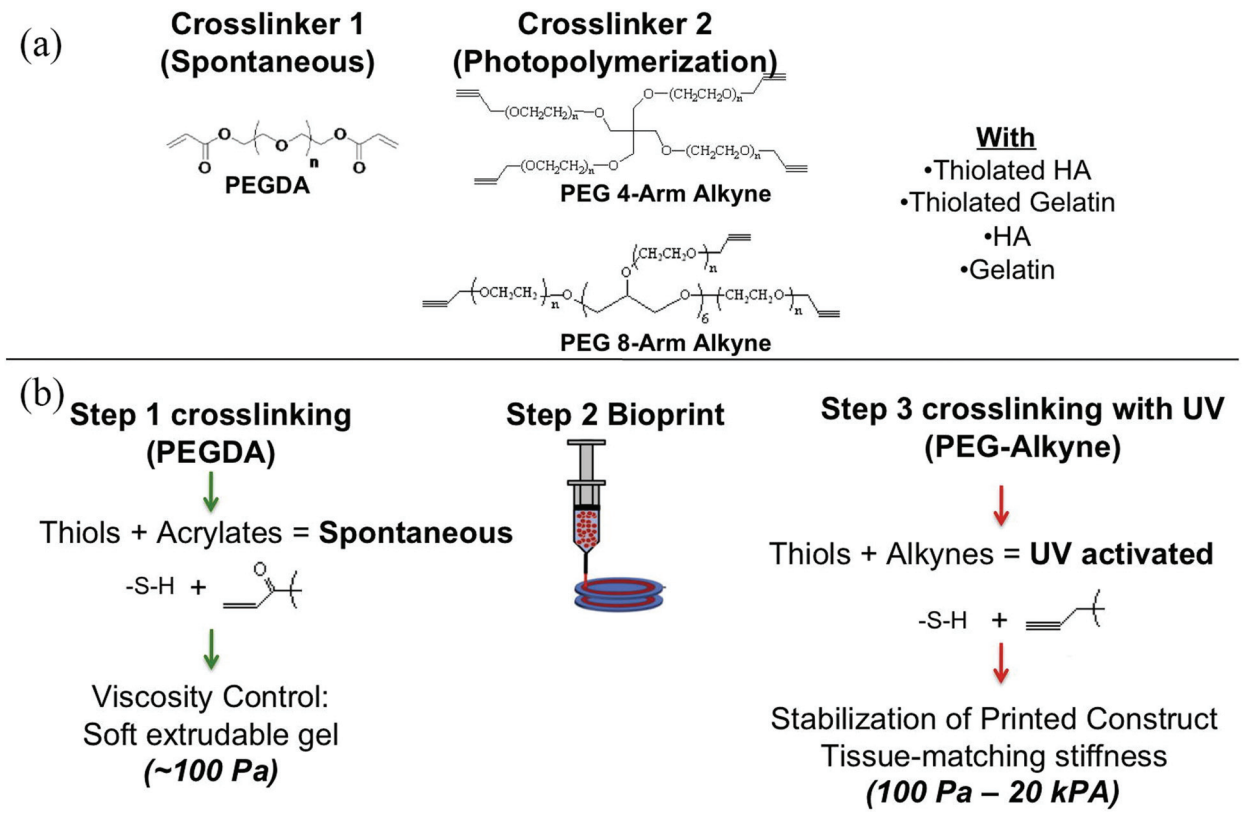

Fig. 10 Employing multiple PEG-based bioinks with tunable cross-linking properties. (a) Strategy of formulation of printable bioinks comprised of acrylate-based cross-linkers (crosslinker 1), alkyne-based cross-linkers (crosslinker 2), thiolated HA, thiolated gelatin, and unmodified HA and gelatin. (b) Implementation of bioprintable hydrogel bioinks: the bioink formulation was prepared and spontaneously cross-linked through thiol-acrylate binding, resulting in a soft, extrudable material. Lastly, the bioprinted structures were fused, stabilized, and brought to the target stiffness.[101] Reprinted with permission Copyright Elsevier, 2015.

found that with this modification, the PEG became the cross-linker for various natural materials *via* the conjugated amine groups (Fig. 11). They successfully established processes for bioprinting PEGX-PEG, PEGX-gelatin, PEGX-gelatin-fibrinogen, and PEGX-gelatin-atelocollagen bioinks containing different types of cells. The results suggested that the PEG modification process is a valuable tool to tune the bioink's properties, increase the bioink options, and to control the cell responses. Similar to gelatin, PEG can also be used in a photopolymerizable form, such as PEGDA, and can be cross-linked *via* light irradiation. Skardal *et al.* used 4-arm PEG-tetracrylate (PEGTA) as a bioink that was cross-linked with thiolated polymers and then compared its performance with PEGDA.[110] In this study, the PEG derivatives were blended with HA and gelatin and cross-linked with the amine groups of these polymers, leading to the bioprinting of stiffer tubular constructs. They concluded that the PEGTA form displayed better results than PEGDA in terms of the rheological properties and extrusion ability and also had better cell response for certain cell types. Moreover, these properties could be further tailored by changing the molecular weight of PEG. The cross-linking of PEGTA is a simple method and seems promising for preparing new bioink formulations. In another study, PEGDA was used as a bioink for bioprinting bone tissue constructs.[111] For the encapsulation of MSCs, the group used PEGDA alone or PEGDA mixed with bioactive glass (BG), HAp, or BG-HAp and compared the cellular performance in these bioinks. The bioprinted PEGDA-HAp constructs showed better bone tissue functionality than PEGDA-BG with respect to ALP activity and collagen secretion, together with higher cell viability and mechanical strength. Recently, Hong *et al.* blended PEGDA with alginate as the bioink and utilized both chemical and ionic cross-linking to significantly enhance the mechanical properties of the bioprinted constructs.[112] They also encapsulated MSCs in this bioink and obtained tough and stretchable cell-laden constructs using dual cross-linking. They successfully bioprinted various sophisticated 3D shapes, including ear, nose, and hollow cubes, where all the constructs showed good cell survival properties (Fig. 12).

Standardization of the evaluation of the printing and of the rheological properties is a critical need in bioprinting. Recently, a few studies were focused on the printability and rheological properties of PEG-based and/or poloxamer-based bioinks. Poloxamers are block copolymers of PEG and poly(propylene glycol) (PPG).[113] In one study, poloxamer 407, a commercially available hydrophilic non-ionic surfactant,

Published on 01 2018. Downloaded on 22.5.2025 22:31:12.

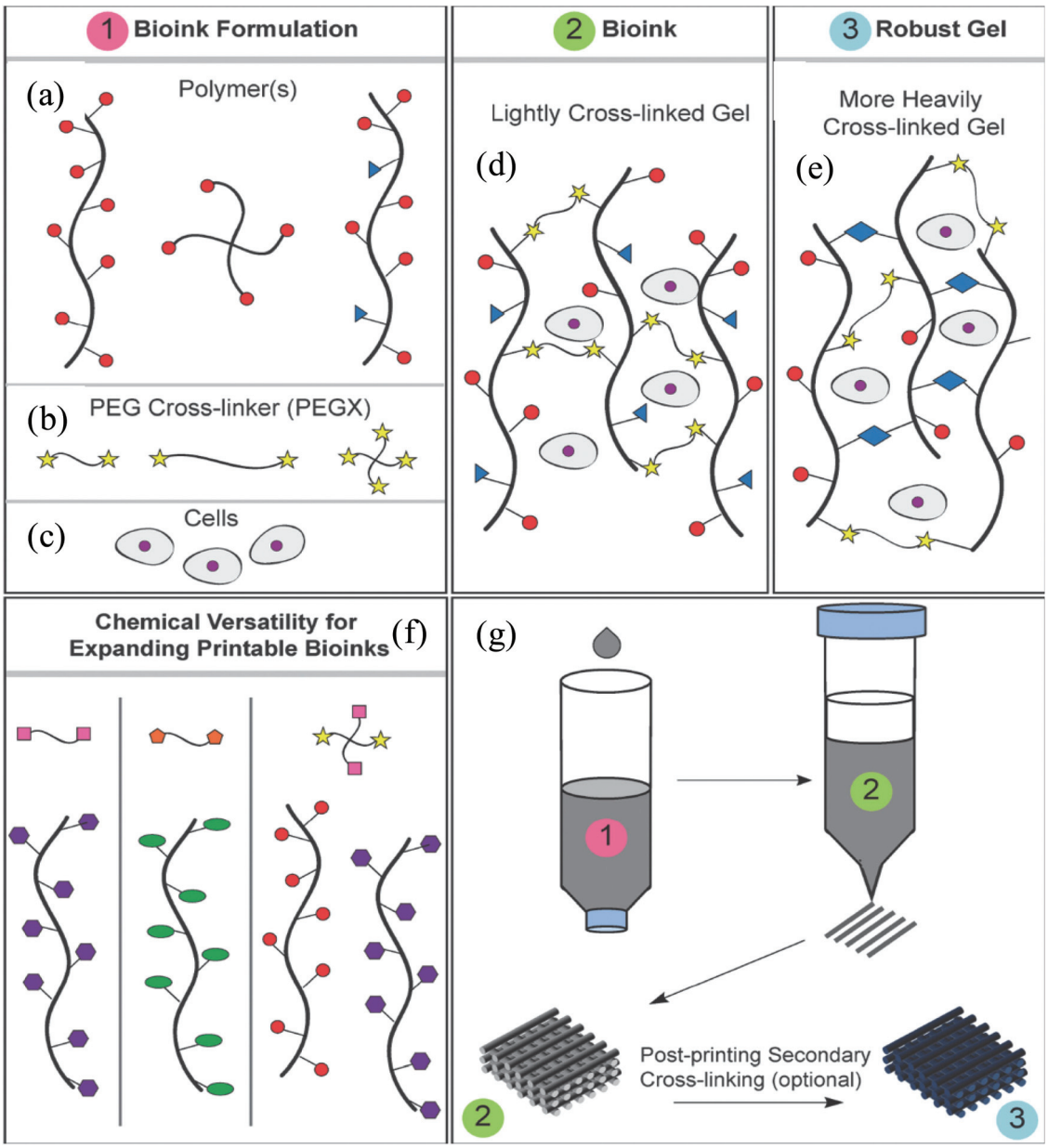

Fig. 11 PEG-based cell-laden bioinks. (a) Polymer or polymer mixtures in linear (gelatin), branched (4-arm PEG amine), or multifunctional form. The red circles represent amines, blue triangles represent methacrylate groups, and the yellow stars indicate SVA groups of PEGX. (b) PEGX can be linear or multiarm and can have various chain lengths. (c) Cells can be encapsulated by (d) mixing with polymers and PEGX to form the bioink. (e) Alternatively, secondary cross-linking can be performed to increase mechanical strength following the printing step. (f) By changing the reactive groups of PEGX, polymers of other functional groups can be cross-linked. Purple polygons represent thiols, cross-linkable with maleimide PEGX (pink squares) and green ellipses represent alkynes, cross-linkable with azide PEGX (orange pentagon). (g) Printing process of PEGX bioink method and corresponding phase: PEGX with or without cells were mixed within the polymer solution and loaded into the printing cartridge. After gel formation and stable mechanical properties were achieved, gels could be 3D printed into multilayer constructs.[49] Reprinted with permission Copyright John Wiley & Sons, Inc., 2015.

an alginate-based hydrogel, and an alginate–gelatin composite hydrogel were used to analyze the rheological properties of bioinks.[114] Hydrogels encapsulating MSCs were bioprinted by using a multi-headed 3D extrusion-based bioprinter. A stress ramp was used to evaluate the yield stress of the mentioned bioinks. The rheological behavior of the bioinks was analyzed using a rheometer and a mathematical model. The flow initiation properties, degree of shear thinning, yield stress, cell survival, and recovery behaviors of the bioinks after bioprinting were used to evaluate the rheological properties. The results showed that no significant reduction was observed in cell viability between the high- and low-shear samples during bioprinting, indicating that shear rates of up to 1639 s^{-1} did not impact the cell viability (between bioprinting pressures of

 This journal is © The Royal Society of Chemistry 2018

Published on 01 2018. Downloaded on 22.5.2025 22:31:12.

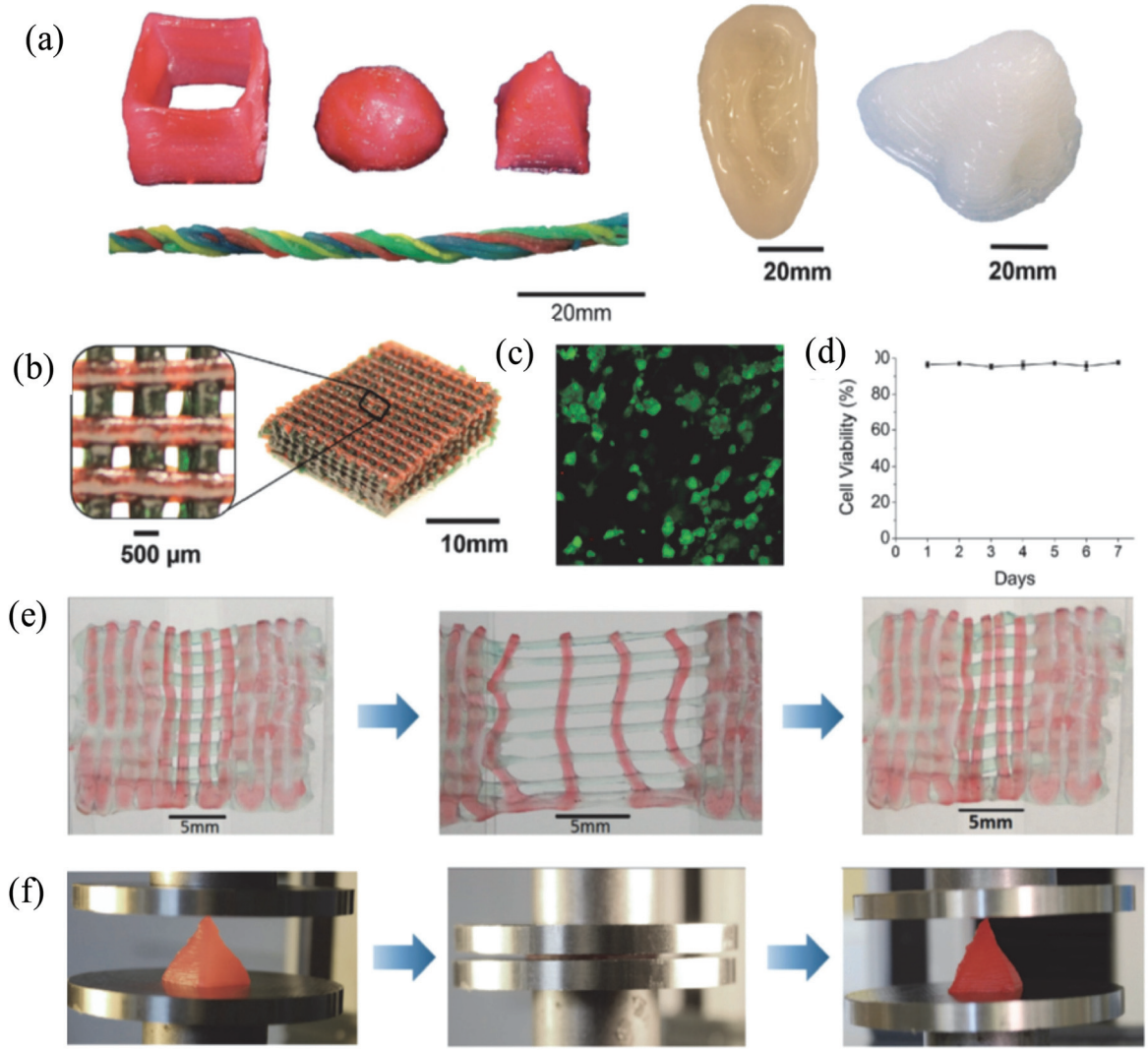

Fig. 12 Rigid and biocompatible PEG-alginate-nanoclay blend bioinks and different 3D bioprinted constructs. (a) Various 3D constructs were printed using a bioink (from left to right: hollow cube, hemisphere, pyramid, twisted bundle, the shape of an ear, and a nose with food dye). (b) A mesh made of hydrogels was printed and was used to host HEK cells. (c) Viability of cells in a collagen hydrogel infused into the 3D printed mesh of the PEG-alginate-nanoclay bioink material. (d) Viability of the cells through 7 d culture. (e) A printed bilayer mesh (top layer red, bottom layer green) was uniaxially stretched up to three times of its initial length. Relaxation of the sample after stretching shows almost complete recovery of its original shape. (f) A printed pyramid underwent a compressive strain of 95% while returning to its original shape after relaxation.[112] Reprinted with permission Copyright John Wiley & Sons, Inc., 2015.

1 bar to 5 bar). It was pointed out that the susceptibility of outer cells at the needle edge would be higher when the shear level was higher than 1639 s^{-1} and therefore this could be the reason for the reduction in cell viability. This study revealed that both the residence time of the cells and the shear rate during bioprinting should be considered to improve cell viability. In another study, an extrusion-based bioprinter was used to evaluate the shape fidelity of bioinks *via* the filament fusion of parallel-bioprinted strands, together with the collapse of the extruded filaments on overhanging structures.[115] Blends of PEG and poloxamer 407-based hydrogels were used to analyze the shape fidelity of bioinks where a rheometer was utilized to carry out rheological studies. The results showed that an increase in the concentration of PEG and at the same time a decrease in the concentration of poloxamer 407 led to a decrease in both yield stress and viscosity of between 30% and 20% of the poloxamer concentration. In the filament collapse test, it was demonstrated that filament bending increased when the gap length was increased. Furthermore, the yield stress increased when the concentration of poloxamer increased, which led to a decrease in bending of the bioprinted constructs. This study revealed that yield stress is an important factor in the shape fidelity of hydrogels after printing. To investigate cell viability during extrusion bioprinting and after bioink curing, Dubbin *et al.* used PEGDA, GelMA, and a novel bioink, recombinant-protein alginate platform for

Published on 01 2018. Downloaded on 22.5.2025 22:31:12.

injectable dual-cross-linked ink (RAPID ink).[116] The recombinant protein, C7 (peptide C), was a component of the RAPID ink and the other component was alginate, which was covalently modified with peptide P. Even though the C and P peptides could form a weak network, the main cross-linking occurred when alginate was exposed to Ca^{2+}. The results showed that less than 10% of the fibroblasts were damaged in the GelMA and PEGDA bioinks; however, in the RAPID bioink, fewer than 4% of the cells were damaged during bioprinting. In addition, it was demonstrated that more than 50% of the cells at the edges of the bioprinted GelMA and PEGDA droplets were damaged after UV light exposure for 5 min. On the other hand, less than 20% of the cells were damaged on the edges of the RAPID bioink after 5 min of exposure in a $CaCl_2$ solution. The observation of reduction in cell death during exposure to a $CaCl_2$ solution was explained by possible prevention of cell dehydration in the solution.

Pluronic is a type of poloxamer and is utilized as a material in bioprinting for generating sacrificial structures.[39] It has good printability and temperature-responsive gelation that are well-suited for use in bioinks.[15] As such, Pluronic can be easily washed away after printing if necessary, as it liquefies at a temperature of 4 °C or lower.[15] While Pluronic has been widely used as sacrificial bioink, its biocompatibility is not sufficient to support long-term cell survival, which limits its direct use as a regular bioink for cell culture. In a recent study, Müller *et al.* reported a strategy termed nanostructuring, which enabled increasing the biocompatibility of Pluronic.[117] In this method, they mixed acrylated and unmodified Pluronic and then removed the unmodified molecules after UV cross-linking, resulting in a significant increase in the viability of the encapsulated chondrocytes of up to 2 weeks in culture due to the increased porosity with the removal. On the other hand, the mechanical strength of the fabricated construct was found to be low, but could be successfully increased by the addition of HAMA. These results suggested that Pluronic can be potentially combined with various polymers and utilized for the bioprinting of different tissue constructs.

In addition to PEG and Pluronic, there are some other synthetic hydrogel-forming polymers that have been used as bioinks in recent studies. In one of these investigations, methacrylated poly[*N*-(2-hydroxypropyl)methacrylamide mono/dilactate] (pHPMA-lac)/PEG triblock copolymers were mixed with HAMA and used as a bioink.[118] This bioink was utilized for the optimization of cartilage-like tissue formation, and PCL was also used for mechanical support during bioprinting. A commercial extrusion-based bioprinter (3D Discovery bioprinter), which had pneumatic robotic dispensers, was used for bioprinting the constructs. In addition to varying the internal geometries *via* bioprinting, different variations and concentrations of these polymers were tested and it was found that there was a dose-dependent effect of HA on the ECM production of chondrocytes. Their observations showed that pHPMA-lac-PEG hydrogels with 0.5% HAMA were optimal for cartilage-like tissue regeneration. Co-printing the hydrogel with PCL and the presence of HAMA increased the stiffness of the constructs to a value close to that of the native cartilage. In another paper, thiol-functionalized HA cross-linked with allyl-functionalized poly(glycidol)s (P(AGE-*co*-G)) was used as a bioink to obtain constructs of articular cartilage tissue.[119] Poly(glycidol)s (PG) have a similar chemical structure to PEGs but possess extra side groups, which enables additional functionalization. For the bioprinting process, an extrusion-based bioprinter was used. It was found that PG-based bioinks combined with HA showed an improvement in cell viability and differentiation with respect to the PG-only bioinks. In a recent study, polyvinylpyrrolidone (PVP) was investigated as a bioink candidate.[120] Different concentrations of PVP (0–3% w/v) were used for bioprinting the constructs with a commercial inkjet bioprinter (RegenHU Biofactory). Their results proved that the addition of PVP improved the printability of the cell mixture. Furthermore, PVP displayed a positive impact on the survival and homogenous dispersion of the bioprinted cells. This study was the first to use PVP as the bioink.

2.5. Commercial bioinks

There are a few commercial biomaterials that have been recently introduced. For instance, Dermamatrix is a commercial natural biomaterial. It is derived from human skin as an allograft consisting of acellular dermis, and it has been used as a biopaper in bioprinting.[121] Another commercial hydrogel is NovoGel, which is a biologically inert material, and this was utilized in bioprinting processes, whereupon printed sacrificial rods formed vessel-like channels[122] similar to the use of agarose rods,[38] or as a printed supportive material for the simultaneous deposition of vessel-mimicking constructs.[123]

More recently, another commercial bioink named CELLINK was introduced. The company provides application-specific, ready-to-use bioinks, on demand. Some of the types of CELLINK bioinks are composed of GelMA, alginate and highly hydrated cellulose nanofibrils, calcium and phosphorous, PCL and Pluronic. Their promise in bioprinting applications were demonstrated in some recent studies. For instance, anatomically shaped cartilage structures were bioprinted successfully and chondrocytes exhibited higher viability rates during the culture period[124–126] and supported redifferentiation of the cells and the synthesis of cartilage ECM.[126]

3. Cell aggregate/pellet-based bioinks

It is becoming increasingly common to use cell pellets or aggregates to prepare bioinks to carry out scaffold-free tissue fabrication. For example, spherical aggregates of Chinese hamster ovary (CHO) cells were prepared and dispensed into micropipettes.[22] In this study, the micropipettes served as cartridges for the bioprinter. During the bioprinting process, one cartridge contained cellular aggregates and another contained collagen gel as the matrix material. A square collagen bed was first created by the bioprinter, and then the cell aggregates were bioprinted into the collagen bed in a square or hexagonal

 This journal is © The Royal Society of Chemistry 2018

Published on 01 2018. Downloaded on 22.5.2025 22:31:12.

shape. CHO cells were also used in another bioprinting study by the same research group.[21] In this work, the cell pellets were first transferred into capillary tubes to form firm cylinders of cells; the cylinders were then removed from the capillary tubes and cut into fragments. Fragments of the cell pellets were subsequently placed on a gyratory shaker inside a cell culture medium to prepare spherical aggregates. Commercial NeuroGel (a biocompatible porous poly[*N*-(2-hydroxypropyl) methacrylamide] hydrogel) disks containing RGD and collagen type I were bioprinted with the cell aggregates. Staining results showed minimal cell death after the fusion of aggregates. The same group also used chicken cardiomyocytes, CHOs, and human vascular endothelial cells to prepare spheroidal bioinks.[127] The aggregates of a mixture of cardiac and endothelial cells were bioprinted onto the collagen gel matrix containing VEGF. Synchronous beating was observed 90 h post-bioprinting. Fig. 13 shows the bioprinting process of the spheroidal bioinks.[128]

Similarly, cell pellets formed from CHOs were used as a bioink, whereby a thermal inkjet bioprinter and ink cartridge were used for depositing cell pellets on collagen type I biopaper.[23] In the apoptosis study, it was observed that there was no significant difference in viability ratios between printed and non-printed cells; in both cases the cell viabilities were close to 90%. A thermal inkjet bioprinter was further used to print cell aggregates from murine MSCs and non-metastatic murine mammary cancer cell lines.[129] During the bioprinting process, ethylenediaminetetraacetic acid (EDTA) was used to avoid salt crystallization as well as cell aggregation. Cell viability studies showed that the addition of EDTA did not cause significant cell death. Cell pellets containing MSCs and Schwann cells with a ratio of 90% to 10% were transferred into capillary tubes and extruded into wells molded from agarose.[130] The cellular cylinders were bioprinted by using a bioprinter with a geometrical structure customized to study a rat sciatic nerve injury model. *In vivo* results demonstrated that there was an extensive axonal re-growth at both the proximal and distal ends of the nerve conduit through the bioprinted grafts. Pellets of mouse embryonic fibroblast cells were transferred into tubes and then transferred into glass capillaries by a continuous bioprinting process (Fig. 14).[123] To analyze apoptosis during bioprinting, apoptotic cell markers were examined with immunoblotting. It was shown that there was no activation of caspase-3 in the continuously bioprinted bioink of ring-shaped cells where caspase-3 was used as an apoptotic cell marker.

Spheroids of human embryonic stem cells could be bioprinted as well. For example, they were deposited with a

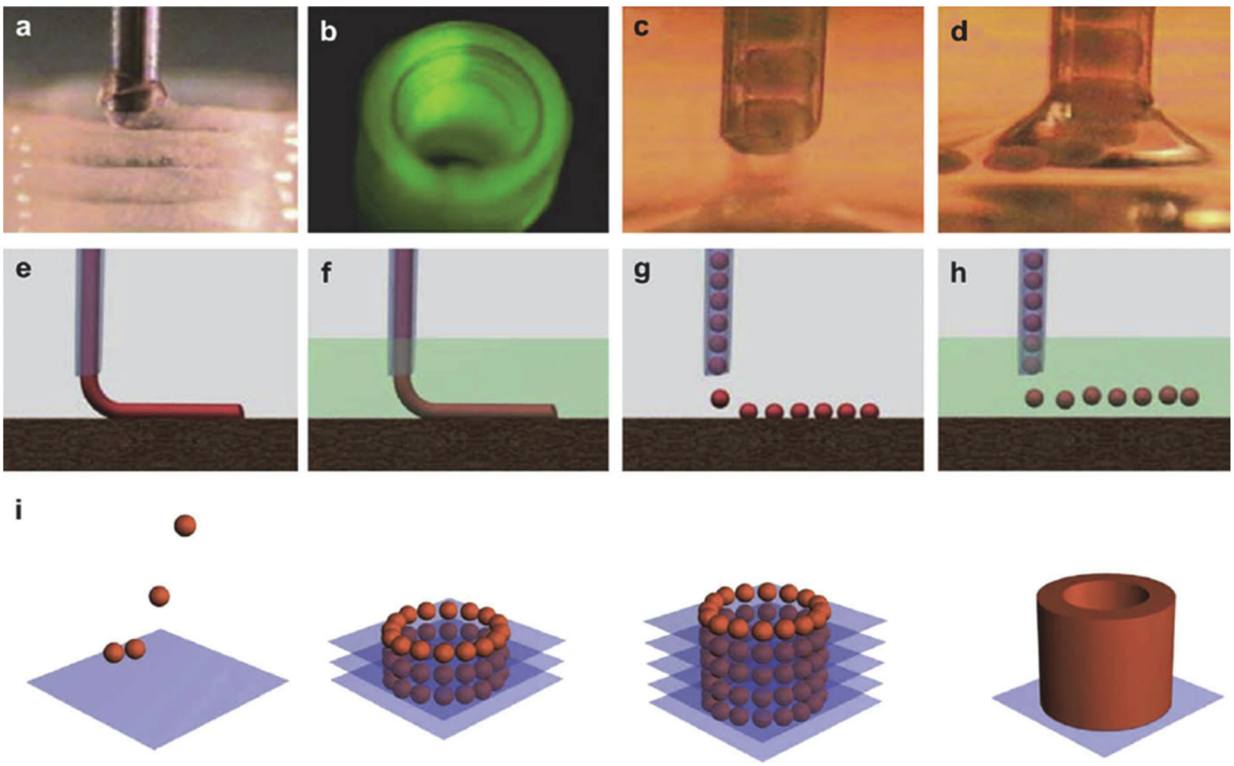

Fig. 13 Use of cell-aggregate-based bioinks and related bioprinting strategies. (a) Bioprinter (general view); (b) multiple bioprinter nozzles; (c) tissue spheroids based bioink before dispensing; (d) tissue spheroids during dispensing; (e) continuous dispensing in air; (f) continuous dispensing in fluid; (g) digital dispensing in air; (h) digital dispensing in fluid; (i) scheme of bioassembly of tubular tissue constructs using bioprinting of self-assembled tissue spheroids illustrating sequential steps of layer-by-layer tissue spheroid deposition and tissue fusion processes.[128] Reprinted with permission Copyright Elsevier, 2009.

Published on 01 2018. Downloaded on 22.5.2025 22:31:12.

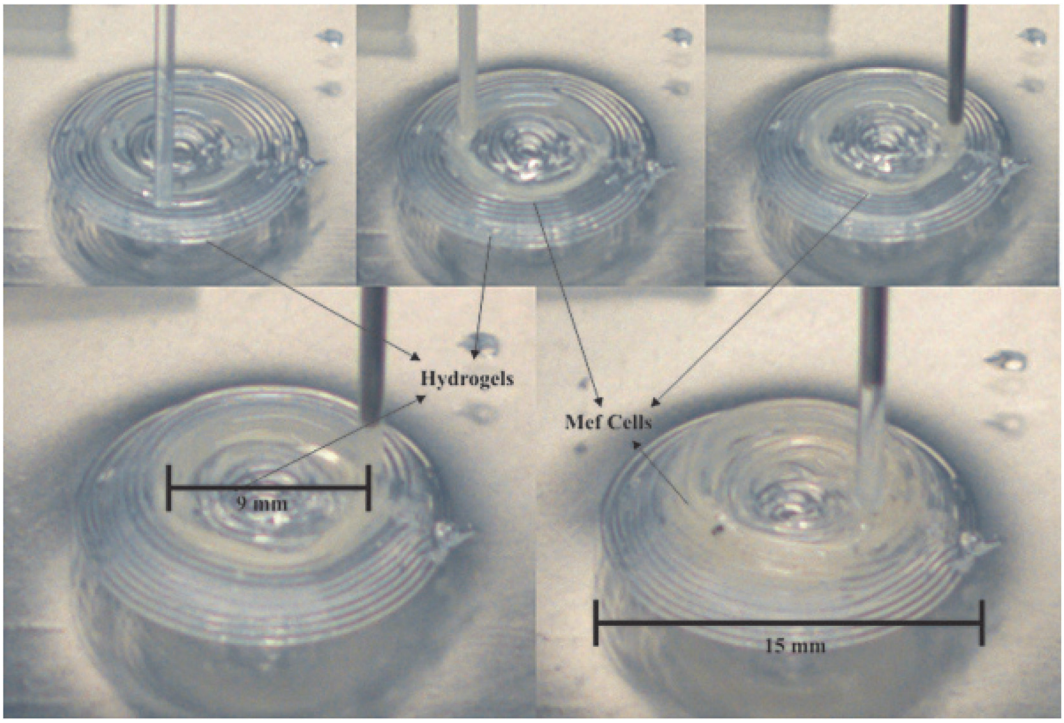

Fig. 14 Aggregate of MEF cells used as a bioink for bioprinting an aorta-like structure while the hydrogel served as a support.[123] Reprinted with permission Copyright John Wiley & Sons, Inc., 2015.

double nozzle system using two different bioink formulations, where one bioink included human embryonic stem cells in the medium and the other one only included the medium.[131] Cells were cultured in a medium without growth factors during spheroid aggregate formation, but after formation of the aggregates, the medium with growth factors was used to induce differentiation. Aggregates of mouse cardiac valve interstitial cells, MSCs, and dermal fibroblasts were formed by using a hanging-drop method and incubated with TGF-β1 or serotonin for 7 days.[132] After 7 days, the differentiated aggregates were placed in contact with each other to allow fusion. It was observed that the aggregates treated with growth factors had higher fusion capacity than those without the treatment of growth factors. Norotte *et al.* used CHOs, SMCs, and fibroblasts to obtain vascular constructs without scaffolds.[133] A custom-made bioprinter with four cartridges was used to prepare vascular structures, while spheroidal or cylindrical vascular constructs were obtained by using multicellular aggregates. Finally, the use of a quantitative system was suggested for rational design of the bioprinting parameters to improve cell viability and cell attachment.[134] Murine MSCs and non-metastatic murine mammary cancer cell lines were bioprinted on collagen to demonstrate the effectiveness of the system. The bioprinted structures were compared with predictions of the quantitative system and it was concluded that the proposed system worked properly for bioprinting applications.

4. Composite bioinks/bioinks with bioactive molecules

4.1. Composite bioinks

Nanomaterials have numerous attractive features and several investigators have combined them into hydrogel biomaterials for making bioinks. Skardal *et al.* used AuNPs as a bioink component and exploited their thiophilicity. These nanoparticles have an affinity to thiol-containing ligands making them multivalent cross-linkers for thiolated molecules.[86] The group blended AuNPs with thiolated HA and gelatin and encapsulated fibroblasts to bioprint vascular structures by using an extrusion-based bioprinter. The Au–thiol bonding was a slow, reversible, and dynamic process with the availability of large regions of interaction sites, which enabled more control over the bioprinting process and over the mechanical strength of the resulting constructs. As expected, fabricated hybrid constructs showed good cell response. Another study utilized silver nanoparticles (AgNPs) for bioprinting a 3D bionic ear.[135] They combined biological and conductive materials to obtain a cyborg organ by employing an extrusion-based commercial bioprinter. They used alginate as the base material for the bioink and mixed it with AgNPs due to their electrical conductivity and then encapsulated chondrocytes as the functional cells. Results suggested that the bioprinted ears were able to receive electromagnetic signals, whereas the encapsulated cells

 This journal is © The Royal Society of Chemistry 2018

Published on 01 2018. Downloaded on 22.5.2025 22:31:12.

were found to be metabolically active. Another study established iron oxide magnetic nanoparticles as a bioink additive, where the researchers mixed these particles with alginate, thereby allowing for additional control over the bioink microarchitecture during bioprinting using a magnetic field.[78,136] They found that the nanoparticles changed the viscosity of the bioink depending on their concentration and that the viscosity affected the nanoparticle movement. They encapsulated endothelial cells within the bioink and investigated their survival rates while changing the bioprinting parameters. They observed that the viability within the first 36 h did not change for the bioprinted cells without nanoparticles but the cell viability decreased for the bioprinted constructs with the nanoparticles. Consistent with the previous studies, increasing the bioprinting pressure negatively affected the cell survival rates, whereas the nozzle size did not have a clear influence on these rates. On the other hand, the group observed that the viability of the encapsulated cells bioprinted with and without nanoparticles using high printing pressures was quite similar, implying that the nanoparticles did not negatively affect the rheological properties of the bioink even at higher concentrations. Importantly, incorporation of the nanoparticles in alginate did not impair the printing resolution, which suggests that they are a good bioink additive, and as a bioink material, it makes them a useful tool for tracking and positioning desired molecules within 3D bioprinted constructs after the printing process.

Nanomaterials have been used for producing conductive bioinks to enhance the signal transduction of embedded cells as well. As an example, DNA was utilized as a surfactant to disperse carbon nanotubes (CNTs) in GelMA or HA to create biocompatible CNT-based bioinks (Fig. 15).[137] Cytotoxicity and cell viability results showed that the cardiomyocytes showed 90% cellular viability after seeding on the printed ink. The immunostaining results of f-actin revealed that the cells had normal cell morphology and adhered well to the printed ink. In addition, the cells that proliferated on conductive bioinks showed high expressions of sarcomeric α-actinin and connexin-43, which are cardiomyocyte specific markers. It is also noteworthy that these conductive bioink formulations showed no toxicity to the cells and also had superior electrical properties that promoted the functions of the cardiomyocytes.[137] Alternatively, bioinks blended with gold nanorods (AuNRs) have also been shown to improve cardiac functions.[138]

Another class of nanomaterials is based on minerals. For example, HAp has been mainly used in bone tissue engineering due to its supportive functions for bone growth and osseointegration. HAp is a calcium phosphate mineral very similar to the inorganic components in bones in mammals.[139,140] Furthermore, HAp is also utilized in bone bioprinting studies as an osteogenic inducer. Gao *et al.* used a thermal inkjet printer with hMSCs suspended in PEG-dimethacrylate nanoparticles of BG or HAp.[111] In the study that used HAp, the cells showed the highest viability, and also the compressive modulus of the constructs was higher. The contents of collagen and ALP were observed to be the highest. In another report, bone morphogenetic protein-2 (BMP-2)-incorporating gelatin microparticles were bioprinted with goat multipotent stromal cell-encapsulating alginate and a mixture of HAp and tricalcium phosphate to evaluate the release of BMP-2 and osteogenic tissue formation.[104] A layer-by-layer bioprinting was carried out by a pneumatic dispensing system. Immunohistochemical staining results demonstrated that in the fast growth factor releasing group, osteocalcin expression was lower than in the slow growth factor releasing group. However, micro-computed tomography (micro-CT) results showed that the duration of the growth factor release time did not change the bone volume significantly. In another study, HAp was mixed with gelatin and alginate, whereupon a two-step mechanism was utilized based on the reversible thermosensitive gelation of gelatin and the irreversible chemical gelation of alginate.[32] During the bioprinting process, a modified 3D bioprinter with two-syringes and a heatable printhead was used. Here, gelatin was used as a short-term stabilizer that was dissolved after a certain time during incubation, where the alginate enabled long-term stability and the HAp was employed for its osteogenic potential (Fig. 16). It was found that the addition of HAp to the gelatin–alginate mixture made the composite more viscous and hence more difficult to print, and the maximum HAp concentration that allowed proper bioprinting was reported as 8%. The results revealed that bioprinted hMSCs showed a high cell viability of 85% after 3 days of subsequent *in vitro* culture even with the higher HAp concentrations. It was also demonstrated that HAp-based bioinks have favorable properties for bone tissue engineering. Catros *et al.* used LaBP while assembling nano-HAp (nHAp) and human osteoprogenitor cells in culture medium.[141] It was demonstrated that LaBP allowed the bioprinting and organization of nHAp and human osteoprogenitor cells in two and three dimensions. In addition, the physicochemical properties of nHAp were preserved during LaBP and cell proliferation was observed for 15 days. In another study, nHAp and sodium alginate were synthesized by wet precipitation.[142] LaBP was utilized by using a laser-induced forward transfer method. In this study, polymers, namely sodium alginate, nano-sized particles, namely nHAp and human endothelial cells were printed with this bioprinting technology. Droplets that are 70 μm in diameter were obtained, with five to seven living cells encapsulated in each droplet.

4.2. Bioinks with bioactive molecules

Biomolecules can be blended into bioinks as well. Growth factors are generally referred to as a group of proteins or steroid hormones that stimulate cell differentiation, proliferation, survival, and tissue regeneration. They can be produced by different types of cells, tissues, and glands.[143–145] In general, certain groups of growth factors act on specific type of tissues, such as the BMP family, which stimulates bone-related processes whereas the VEGF is known to stimulate the vascularization process. For this reason, they are widely used in tissue engineering, either as direct additives inside the scaffold material or entrapped in a controlled release system,

Published on 01 2018. Downloaded on 22.5.2025 22:31:12.

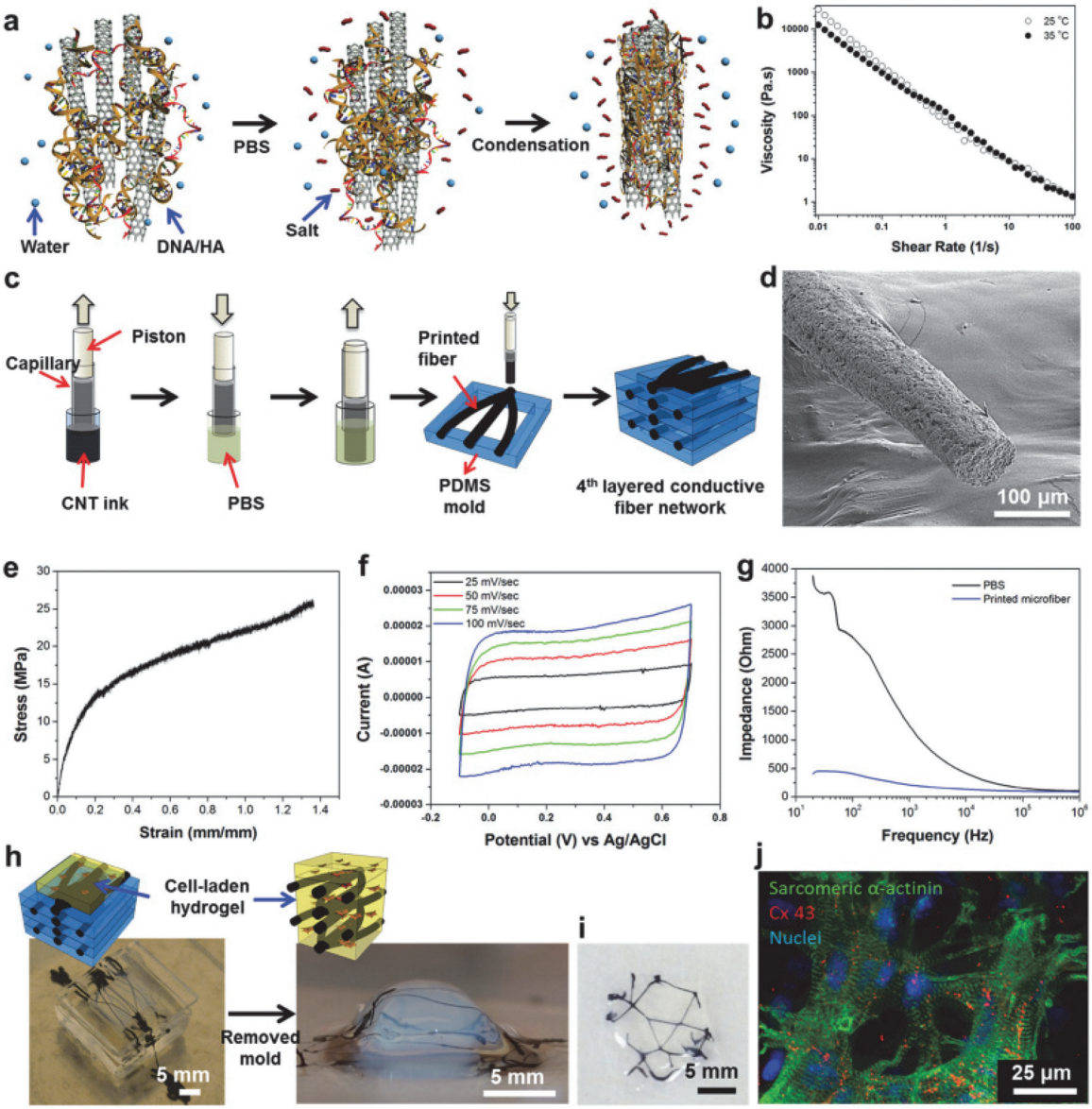

Fig. 15 Preparation and generation of a conductive bioink. (a) A scheme of coagulation reaction of DNA/HA-coated CNT-based bioinks. (b) Viscosity results of a conductive CNT-based bioink. (c) 3D printing of a bioink on a PDMS mold. (d) SEM image shows porous structure of the printed samples. (e) Mechanical test results of printed fibers after swelling. (f) Cyclic voltammetry curves of printed fibers in PBS. (g) Impedance measurements of printed CNT-based microfibers in PBS. (h) Structure of printed fibers inside cell-laden GelMA hydrogels. (i) Top view of GelMA hydrogel shows the printed fibers inside the construct. (j) Immunostaining results of cardiomyocytes encapsulated in GelMA after 10 days including printed fibers for sarcomeric α-actinin (green), cell nuclei (blue), and Cx-43 (red).[137] Reprinted with permission Copyright John Wiley & Sons, Inc., 2016.

such as microspheres. In several studies growth factors were added to the bioink and used in bioprinting applications to stimulate the engineered tissues. Insulin-like growth factor II (IGF-II)-, BMP-2-, and fibroblast growth factor-2 (FGF-2)-containing bioinks were printed on fibrin-coated surfaces with an inkjet deposition system.[146] Myogenic cells were then seeded on the printed structures. Desorption experiments performed with IGF-II and BMP-2 showed that the growth factors were retained on the samples in serum-containing medium after 10 days. Studies with myogenic cells on the printed BMP-2 samples showed that there was a notable increase in their ALP expression levels; however, on the control and FGF-2 samples, there was no noticeable expression of ALP. Similarly, Cooper *et al.* used an inkjet deposition system to bioprint human recombinant BMP-2, noggin, growth and differentiation factor-5 (GDF-5), and transforming growth factor-β1 (TGF-β1) on human acellular dermis.[121] Myogenic precursor cells were seeded on growth factor-containing substrates. The bioprinting of BMP-2 was done on one half of the circular acellular dermis, whereas the other part was left empty or bioprinted with noggin, GDF-5, or TGF-β1. Histological analysis showed that human acellular dermis alone did not stimulate the for-

 This journal is © The Royal Society of Chemistry 2018

Published on 01 2018. Downloaded on 22.5.2025 22:31:12.

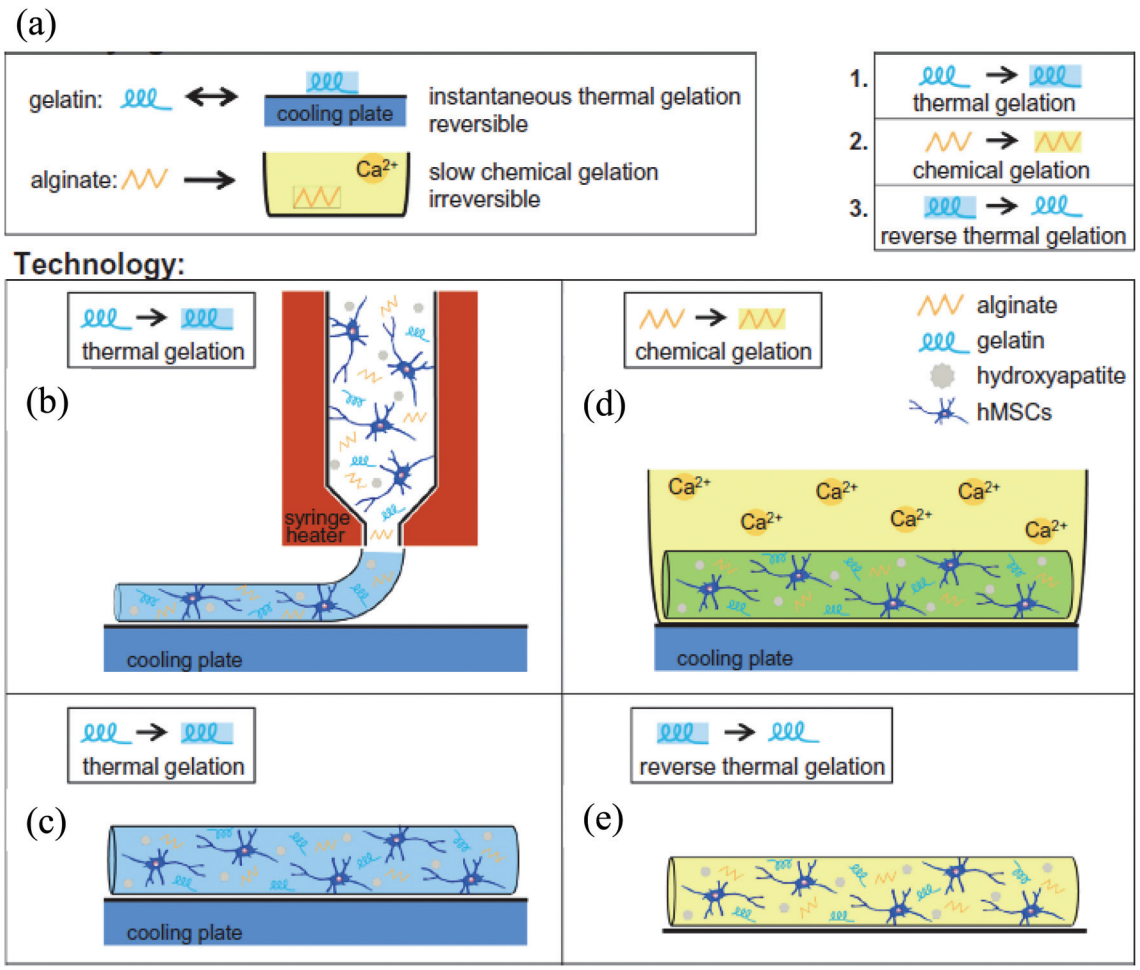

Fig. 16 (a) Schematic diagrams of the two-step gelation mechanism of bioinks: thermoresponsive gelation of gelatin and the irreversible chemical gelation of alginate at the polymer level. (b) Printing of heated hydrogel precursor including living cells onto a cold substrate. (c) First gelation step by decreasing the temperature, which resulted in solidification of the gelatin. (d) After printing the whole construct, it was immersed in a $CaCl_2$ solution to cross-link the alginate within the hydrogel precursor mixture. This procedure was performed in a cold environment to preserve the stability of the construct until chemical cross-linking was completed. (e) Long-term stability was ensured by the cross-linked alginate and then the cooling plate was removed.[32] Reprinted with permission Copyright Elsevier, 2014.

mation of bone tissue, whereas new bone-like structures were formed on the BMP-2 printed sections of the construct.

Blood plasma is the ECM of blood cells consisting of a solution of salts and proteins such as fibrinogen, albumin, and globulin.[147] Due to its advantage of being a natural mixture of vital proteins and minerals, blood plasma has been utilized as a bioink. Gruene *et al.* combined blood plasma with alginate for encapsulating ASCs, and fabricated 3D multilayer grafts by using the LaBP technique.[148] Experiments revealed that the proliferation and differentiation ability of the stem cells were preserved after the bioprinting process. Another study utilized the same bioprinting procedure and the same blood plasma–alginate bioink mixture for skin tissue engineering.[16] They were able to build layered structures where every single layer was patterned with different cell types, and proper cellular functionality and intercellular junction formation were observed after bioprinting.

A novel cryo (freezing) bioink was reported by El Assal *et al.*, where red blood cells (RBCs) were bioprinted as nanodroplets for cryopreservation.[149] The cryo bioink included PEG, ectoine, and trehalose molecules and served as a protective solution for RBCs during cooling and thawing processes. The optimum concentrations of the cryo bioink components were found through experiments. The extrusion-based bioprinting system enabled the dispensing of RBC-laden cryo bioink in the form of droplets. The results revealed that the cellular morphology and functions of the bioprinted patterns were successfully maintained.

Besides proteins, ultrashort peptides, including trimer, tetramer, and hexamers, were proposed as composite bioink materials, and the parameters critical for bioprinting were next evaluated.[12] These materials were soluble in water even at low temperatures and possessed stimuli-responsive gelation and self-assembly properties, enabling them to obtain rigid

Published on 01 2018. Downloaded on 22.5.2025 22:31:12.

hydrogels with good shape fidelity and a stiffness of around 40 kPa, which is one order of magnitude greater than that of other short-peptide-based hydrogels. Thanks to their amphiphilic structure, they could hold a large amount of water for protecting cells from dehydration during the bioprinting process. Furthermore, human MSCs encapsulated in peptide hydrogel droplets exhibited alignment and elongation in less than a week and the 3D constructs presented good *in vivo* biocompatibility and stability. With these unique properties, peptide bioinks are not only suitable bioink materials for tissue engineering but also favorable bioinks for drug delivery and therapeutics screening applications.

Microbes may also function as bioinks. For example, genetically engineered phage was recently introduced as a new bioink material due to its tailorable design at the molecular level, which enabled the research team to add the desired properties for bioprinting applications.[13] Specifically, M13 phages with their integrin-binding (GRGDS) and calcium-binding (DDYD) domains on their surfaces were mixed with alginate for proper cross-linking in the presence of Ca^{2+} ions (Fig. 17). Preosteoblasts were encapsulated in this bioink and bioprinted with a computer-controlled three-axis robotic system and a dispenser. Bioprinted cell-laden constructs displayed higher levels of cell viability, proliferation, and differentiation than those encapsulated in pure alginate, implying a strong potential of creating bioinks from engineered phages. Similar to peptide bioinks, the self-assembly property, replicability, and tunable design at the molecular level are outstanding properties which can pave the way to create new bioinks in a similar manner and could further accelerate bioprinting applications.

5. Future remarks

Bioprinting is a promising strategy to engineer 3D tissue constructs with precisely defined structures and geometries by using living cells and biomaterials. Bioinks are an essential component of bioprinting and typically consist of biomaterials (such as hydrogels), cells, or cell aggregates, or their combinations. Several natural (*e.g.*, alginate and gelatin) and synthetic (*e.g.*, PCL, PEG, Pluronic) polymers have been utilized as bioinks. Although there are numerous efforts on the advancement of the bioprinting technology, the development of appropriate bioinks that satisfactorily meet bioprinting requirements with regards to the mechanical, rheological, and biological properties have been limited to date. Thus, the development of new bioink materials and the engineering of novel bioink formulations are currently major areas of interest. In addition, more work is needed in creating models and standards to compare and to evaluate the properties of different bioink materials. To this end, new metrics need to be developed for evaluating bioinks and bioprinting processes, which are very important to standardize their uses. As we mentioned above, a pioneering work has established a method to evaluate the shape fidelity of bioinks *via* the filament fusion of parallel-bioprinted strands using an extrusion bioprinter, as well as the filament collapse on overhanging structures.[115] In

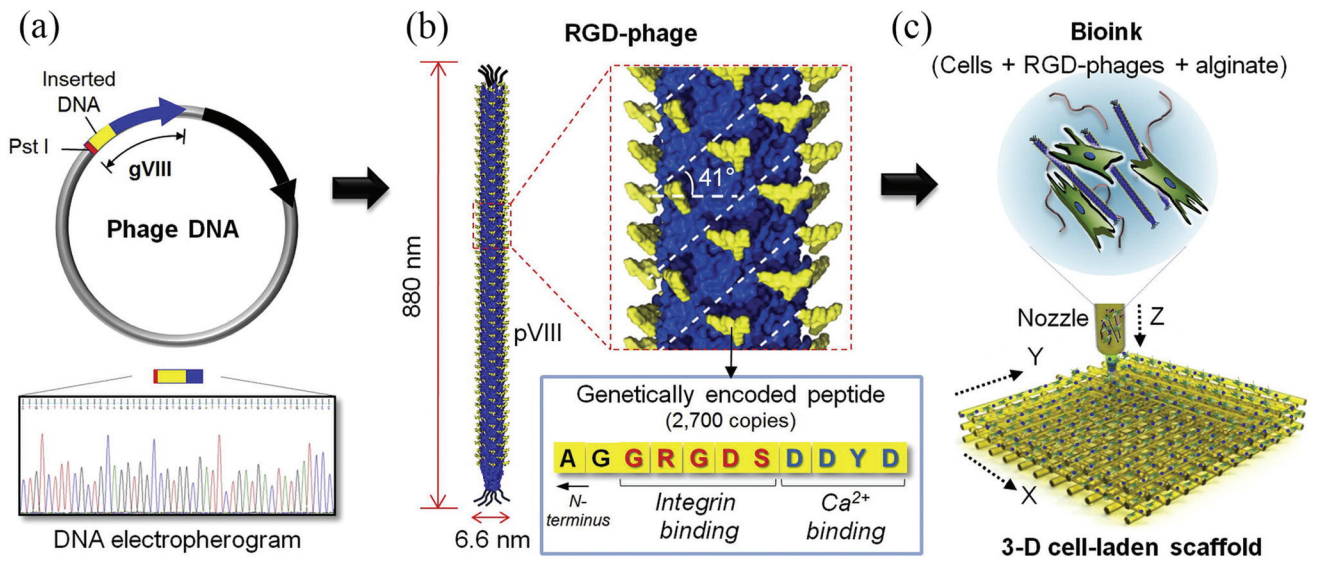

Fig. 17 The use of phages as a nanobioink. The nano-filamentous M13 bacteriophage was genetically engineered to present cell-adhesive peptides on its major protein. (a) Target genes were inserted into the gVIII region, leading to close proximity to the N-terminus of pVIII. The resulting circular DNA was then transformed into *E. coli*, creating the engineered M13 phages, which were identified by DNA sequencing. (b) Schematic diagram of an M13 phage displaying a regularly spaced, dense array of biochemical motifs, including both the integrin-binding segment (GRGDS) and the Ca^{2+}-binding segment (DDYD). (c) Schematic diagram of a bioink (target cells + RGD-phages + alginate) and a 3D cell-laden construct printed using the phage-based bioink.[13] Reprinted with permission Copyright Elsevier, 2016.

 This journal is © The Royal Society of Chemistry 2018

addition, the development of new computational models is another area of interest to fully analyze the printability and behaviors of the bioinks prior to experimental optimizations. In view of the above-mentioned topics, this review has provided in-depth details about the current bioinks and it is anticipated that this will benefit the broad readership in the field of bioprinting and tissue engineering.

Conflicts of interest

The authors declare no conflict of interests in this work.

Acknowledgements

P. S. G. O. acknowledges funding (B.14.2.TBT.0.06.01-219-115543) and I. I. acknowledges funding (B.02.1.TBT.0.06.01-219-115543) from the Scientific and Technological Research Council of Turkey (TUBITAK). This work was supported by the National Institutes of Health (AR066193, EB021148, EB021857, AR070647, EB023052, CA214411, AR057837, HL137193, and EB024403), the Office of Naval Research PECASE Award, the National Science Foundation (EFRI-1240443), and the Scientific and Technological Research Council of Turkey (TUBITAK). Y. S. Z. acknowledges the National Cancer Institute of the National Institutes of Health Pathway to Independence Award (CA201603) and the Science and Technology Commission of Shanghai Municipality (STCSM) 17JC 1400200.

Published on 01 2018. Downloaded on 22.5.2025 22:31:12.

References

1 P. Bajaj, R. M. Schweller, A. Khademhosseini, J. L. West and R. Bashir, *Annu. Rev. Biomed. Eng.*, 2014, **16**, 247–276.
2 J. Groll, T. Boland, T. Blunk, J. A. Burdick, D.-W. Cho, P. D. Dalton, B. Derby, G. Forgacs, Q. Li, V. A. Mironov, L. Moroni, M. Nakamura, W. Shu, S. Takeuchi, G. Vozzi, T. B. F. Woodfield, T. Xu, J. J. Yoo and J. Malda, *Biofabrication*, 2016, **8**, 013001.
3 S. V. Murphy and A. Atala, *Nat. Biotechnol.*, 2014, **32**, 773–785.
4 Y. S. Zhang, K. Yue, J. Aleman, K. M. Mollazadeh-Moghaddam, S. M. Bakht, V. Dell'Erba, P. Assawes, S. R. Shin, M. R. Dokmeci, R. Oklu and R. A. Khademhosseini, *Ann. Biomed. Eng.*, 2017, **45**, 148–163.
5 Y. S. Zhang, M. Duchamp, R. Oklu, L. W. Ellisen, R. Langer and A. Khademhosseini, *ACS Biomater. Sci. Eng.*, 2016, **2**, 1710–1721.
6 J. K. Carrow, P. Kerativitayanan, M. K. Jaiswal, G. Lokhande and A. K. Gaharwar, in *Essentials of 3D Biofabrication and Translation*, ed. A. A. J. Yoo, Academic Press, Boston, 2015, pp. 229–248.
7 S. Wüst, R. Müller and S. Hofmann, *J. Funct. Biomater.*, 2011, **2**, 119–154.
8 A. B. Dababneh and I. T. Ozbolat, *J. Manuf. Sci. Eng.*, 2014, **136**, 061016–061016.
9 S. Khalil and W. Sun, *J. Biomech. Eng.*, 2009, **131**, 111002.
10 Z. Wang, R. Abdulla, B. Parker, R. Samanipour, S. Ghosh and K. Kim, *Biofabrication*, 2015, **7**, 045009.
11 H. J. Lee, Y. B. Kim, S. H. Ahn, J.-S. Lee, C. H. Jang, H. Yoon, W. Chun and G. H. Kim, *Adv. Healthcare Mater.*, 2015, **4**, 1359–1368.
12 Y. Loo, A. Lakshmanan, M. Ni, L. L. Toh, S. Wang and C. A. E. Hauser, *Nano Lett.*, 2015, **15**, 6919–6925.
13 D.-Y. Lee, H. Lee, Y. Kim, S. Y. Yoo, W.-J. Chung and G. Kim, *Acta Biomater.*, 2016, **29**, 112–124.
14 R. K. Bregg, *Current Topics in Polymer Research*, Nova Publishers, 2005.
15 C. C. Chang, E. D. Boland, S. K. Williams and J. B. Hoying, *J. Biomed. Mater. Res., Part B*, 2011, **98**, 160–170.
16 L. Koch, A. Deiwick, S. Schlie, S. Michael, M. Gruene, V. Coger, D. Zychlinski, A. Schambach, K. Reimers, P. M. Vogt and B. Chichkov, *Biotechnol. Bioeng.*, 2012, **109**, 1855–1863.
17 S. Michael, H. Sorg, C.-T. Peck, L. Koch, A. Deiwick, B. Chichkov, P. M. Vogt and K. Reimers, *PLoS One*, 2013, **8**, e57741.
18 V. Lee, G. Singh, J. P. Trasatti, C. Bjornsson, X. Xu, T. N. Tran, S.-S. Yoo, G. Dai and P. Karande, *Tissue Eng., Part C*, 2014, **20**, 473–484.
19 S. Moon, S. K. Hasan, Y. S. Song, F. Xu, H. O. Keles, F. Manzur, S. Mikkilineni, J. W. Hong, J. Nagatomi, E. Haeggstrom, A. Khademhosseini and U. Demirci, *Tissue Eng., Part C*, 2010, **16**, 157–166.
20 D. F. Duarte Campos, A. Blaeser, A. Korsten, S. Neuss, J. Jäkel, M. Vogt and H. Fischer, *Tissue Eng., Part A*, 2015, **21**, 740–756.
21 K. Jakab, A. Neagu, V. Mironov, R. R. Markwald and G. Forgacs, *Proc. Natl. Acad. Sci. U. S. A.*, 2004, **101**, 2864–2869.
22 K. Jakab, B. Damon, A. Neagu, A. Kachurin and G. Forgacs, *Biorheology*, 2006, **43**, 509–513.
23 X. Cui, D. Dean, Z. M. Ruggeri and T. Boland, *Biotechnol. Bioeng.*, 2010, **106**, 963–969.
24 J. Zhu and R. E. Marchant, *Expert Rev. Med. Devices*, 2011, **8**, 607–626.
25 A. O. Elzoghby, *J. Controlled Release*, 2013, **172**, 1075–1091.
26 Q. Xing, K. Yates, C. Vogt, Z. Qian, M. C. Frost and F. Zhao, *Sci. Rep.*, 2014, **4**, 4706.
27 W. Schuurman, P. A. Levett, M. W. Pot, P. R. van Weeren, W. J. A. Dhert, D. W. Hutmacher, F. P. W. Melchels, T. J. Klein and J. Malda, *Macromol. Biosci.*, 2013, **13**, 551–561.
28 J. W. Nichol, S. T. Koshy, H. Bae, C. M. Hwang, S. Yamanlar and A. Khademhosseini, *Biomaterials*, 2010, **31**, 5536–5544.
29 T. Zhang, K. C. Yan, L. Ouyang and W. Sun, *Biofabrication*, 2013, **5**, 045010.

Published on 01 2018. Downloaded on 22.5.2025 22:31:12.

30 M. Neufurth, X. Wang, H. C. Schröder, Q. Feng, B. Diehl-Seifert, T. Ziebart, R. Steffen, S. Wang and W. E. G. Müller, *Biomaterials*, 2014, **35**, 8810–8819.
31 B. Duan, L. A. Hockaday, K. H. Kang and J. T. Butcher, *J. Biomed. Mater. Res., Part A*, 2013, **101**, 1255–1264.
32 S. Wüst, M. E. Godla, R. Müller and S. Hofmann, *Acta Biomater.*, 2014, **10**, 630–640.
33 K. Yue, G. Trujillo-de Santiago, M. M. Alvarez, A. Tamayol, N. Annabi and A. Khademhosseini, *Biomaterials*, 2015, **73**, 254–271.
34 Y.-C. Chen, R.-Z. Lin, H. Qi, Y. Yang, H. Bae, J. M. Melero-Martin and A. Khademhosseini, *Adv. Funct. Mater.*, 2012, **22**, 2027–2039.
35 H. Shin, B. D. Olsen and A. Khademhosseini, *Biomaterials*, 2012, **33**, 3143–3152.
36 C. B. Hutson, J. W. Nichol, H. Aubin, H. Bae, S. Yamanlar, S. Al-Haque, S. T. Koshy and A. Khademhosseini, *Tissue Eng., Part A*, 2011, **17**, 1713–1723.
37 W. Xiao, J. He, J. W. Nichol, L. Wang, C. B. Hutson, B. Wang, Y. Du, H. Fan and A. Khademhosseini, *Acta Biomater.*, 2011, **7**, 2384–2393.
38 L. E. Bertassoni, J. C. Cardoso, V. Manoharan, A. L. Cristino, N. S. Bhise, W. A. Araujo, P. Zorlutuna, N. E. Vrana, A. M. Ghaemmaghami, M. R. Dokmeci and A. Khademhosseini, *Biofabrication*, 2014, **6**, 024105.
39 D. B. Kolesky, R. L. Truby, A. S. Gladman, T. A. Busbee, K. A. Homan and J. A. Lewis, *Adv. Mater.*, 2014, **26**, 3124–3130.
40 A. Skardal, J. Zhang, L. McCoard, X. Xu, S. Oottamasathien and G. D. Prestwich, *Tissue Eng., Part A*, 2010, **16**, 2675–2685.
41 B. Duan, E. Kapetanovic, L. A. Hockaday and J. T. Butcher, *Acta Biomater.*, 2014, **10**, 1836–1846.
42 A. C. Daly, S. E. Critchley, E. M. Rencsok and D. J. Kelly, *Biofabrication*, 2016, **8**, 045002.
43 R. Levato, W. R. Webb, I. A. Otto, A. Mensinga, Y. Zhang, M. van Rijen, R. van Weeren, I. M. Khan and J. Malda, *Acta Biomater.*, 2017, **61**, 41–53.
44 T. Rajangam and S. S. A. An, *Int. J. Nanomed.*, 2013, **8**, 3641–3662.
45 X. Cui and T. Boland, *Biomaterials*, 2009, **30**, 6221–6227.
46 M. Nakamura, S. Iwanaga, C. Henmi, K. Arai and Y. Nishiyama, *Biofabrication*, 2010, **2**, 014110.
47 T. Xu, K. W. Binder, M. Z. Albanna, D. Dice, W. Zhao, J. J. Yoo and A. Atala, *Biofabrication*, 2013, **5**, 015001.
48 M. Gruene, M. Pflaum, C. Hess, S. Diamantouros, S. Schlie, A. Deiwick, L. Koch, M. Wilhelmi, S. Jockenhoevel, A. Haverich and B. Chichkov, *Tissue Eng., Part C*, 2011, **17**, 973–982.
49 A. L. Rutz, K. E. Hyland, A. E. Jakus, W. R. Burghardt and R. N. Shah, *Adv. Mater.*, 2015, **27**, 1607–1614.
50 C. Vepari and D. L. Kaplan, *Prog. Polym. Sci.*, 2007, **32**, 991–1007.
51 K. Schacht, T. Jüngst, M. Schweinlin, A. Ewald, J. Groll and T. Scheibel, *Angew. Chem., Int. Ed.*, 2015, **54**, 2816–2820.
52 S. Das, F. Pati, Y.-J. Choi, G. Rijal, J.-H. Shim, S. W. Kim, A. R. Ray, D.-W. Cho and S. Ghosh, *Acta Biomater.*, 2015, **11**, 233–246.
53 K. Y. Lee and D. J. Mooney, *Prog. Polym. Sci.*, 2012, **37**, 106–126.
54 Y. Zhang, Y. Yu, A. Akkouch, A. Dababneh, F. Dolati and I. T. Ozbolat, *Biomater. Sci.*, 2014, **3**, 134–143.
55 J. Jia, D. J. Richards, S. Pollard, Y. Tan, J. Rodriguez, R. P. Visconti, T. C. Trusk, M. J. Yost, H. Yao, R. R. Markwald and Y. Mei, *Acta Biomater.*, 2014, **10**, 4323–4331.
56 J. Yan, Y. Huang and D. B. Chrisey, *Biofabrication*, 2013, **5**, 015002.
57 P. de Vos, M. M. Faas, B. Strand and R. Calafiore, *Biomaterials*, 2006, **27**, 5603–5617.
58 Y. A. Mørch, M. Qi, P. O. M. Gundersen, K. Formo, I. Lacik, G. Skjåk-Braek, J. Oberholzer and B. L. Strand, *J. Biomed. Mater. Res., Part A*, 2012, **100**, 2939–2947.
59 Y. Yu, Y. Zhang, J. A. Martin and I. T. Ozbolat, *J. Biomech. Eng.*, 2013, **135**, 91011.
60 Y. Zhang, Y. Yu, H. Chen and I. T. Ozbolat, *Biofabrication*, 2013, **5**, 025004.
61 Q. Gao, Y. He, J. Fu, A. Liu and L. Ma, *Biomaterials*, 2015, **61**, 203–215.
62 H. Gudapati, J. Yan, Y. Huang and D. B. Chrisey, *Biofabrication*, 2014, **6**, 035022.
63 B. Guillotin, A. Souquet, S. Catros, M. Duocastella, B. Pippenger, S. Bellance, R. Bareille, M. Rémy, L. Bordenave, J. Amédée and F. Guillemot, *Biomaterials*, 2010, **31**, 7250–7256.
64 D. Kingsley, A. Dias, D. Chrisey and D. Corr, *Biofabrication*, 2013, **5**, 045006.
65 L. Gasperini, D. Maniglio, A. Motta and C. Migliaresi, *Tissue Eng., Part C*, 2015, **21**, 123–132.
66 S. K. Williams, J. S. Touroo, K. H. Church and J. B. Hoying, *BioRes. Open Access*, 2013, **2**, 448–454.
67 K. Nair, M. Gandhi, S. Khalil, K. C. Yan, M. Marcolongo, K. Barbee and W. Sun, *Biotechnol. J.*, 2009, **4**, 1168–1177.
68 R. Chang, K. Emami, H. Wu and W. Sun, *Biofabrication*, 2010, **2**, 045004.
69 J. Kundu, J.-H. Shim, J. Jang, S.-W. Kim and D.-W. Cho, *J. Tissue Eng. Regener. Med.*, 2015, **9**, 1286–1297.
70 W. Schuurman, V. Khristov, M. W. Pot, P. R. van Weeren, W. J. A. Dhert and J. Malda, *Biofabrication*, 2011, **3**, 021001.
71 C. Xu, W. Chai, Y. Huang and R. R. Markwald, *Biotechnol. Bioeng.*, 2012, **109**, 3152–3160.
72 C. Xu, M. Zhang, Y. Huang, A. Ogale, J. Fu and R. R. Markwald, *Langmuir*, 2014, **30**, 9130–9138.
73 M. Mobed-Miremadi, E. Acks, S. Polsaward and D. Chen, *Artif. Cells, Blood Substitutes, Immobilization Biotechnol.*, 2011, **39**, 310–316.
74 A. H. Bacelar, J. Silva-Correia, J. M. Oliveira and R. L. Reis, *J. Mater. Chem. B*, 2016, **4**, 6164–6174.
75 T. Wuestenberg, *Cellulose and Cellulose Derivatives in the Food Industry: Fundamentals and Applications*, John Wiley & Sons, 2014.

 This journal is © The Royal Society of Chemistry 2018

Published on 01 2018. Downloaded on 22.5.2025 22:31:12.

76 J. T. Oliveira, L. Martins, R. Picciochi, P. B. Malafaya, R. A. Sousa, N. M. Neves, J. F. Mano and R. L. Reis, *J. Biomed. Mater. Res., Part A*, 2010, **93**, 852–863.
77 F. P. W. Melchels, W. J. A. Dhert, D. W. Hutmacher and J. Malda, *J. Mater. Chem. B*, 2014, **2**, 2282–2289.
78 K. Buyukhatipoglu, W. Jo, W. Sun and A. M. Clyne, *Biofabrication*, 2009, **1**, 035003.
79 R. Lozano, L. Stevens, B. C. Thompson, K. J. Gilmore, R. Gorkin III, E. M. Stewart, M. in het Panhuis, M. Romero-Ortega and G. G. Wallace, *Biomaterials*, 2015, **67**, 264–273.
80 J. Visser, B. Peters, T. J. Burger, J. Boomstra, W. J. A. Dhert, F. P. W. Melchels and J. Malda, *Biofabrication*, 2013, **5**, 035007.
81 R. Levato, J. Visser, J. A. Planell, E. Engel, J. Malda and M. A. Mateos-Timoneda, *Biofabrication*, 2014, **6**, 035020.
82 J. Monslow, P. Govindaraju and E. Puré, *Front. Immunol.*, 2015, **6**, 231.
83 P. N. Sudha and M. H. Rose, *Adv. Food Nutr. Res.*, 2014, **72**, 137–176.
84 M. K. Cowman, T. A. Schmidt, P. Raghavan and A. Stecco, *F1000Research*, 2015, **4**, 622.
85 J. Y. Park, J.-C. Choi, J.-H. Shim, J.-S. Lee, H. Park, S. W. Kim, J. Doh and D.-W. Cho, *Biofabrication*, 2014, **6**, 035004.
86 A. Skardal, J. Zhang, L. McCoard, S. Oottamasathien and G. D. Prestwich, *Adv. Mater.*, 2010, **22**, 4736–4740.
87 M. Kesti, M. Müller, J. Becher, M. Schnabelrauch, M. D'Este, D. Eglin and M. Zenobi-Wong, *Acta Biomater.*, 2015, **11**, 162–172.
88 G. Sun and J. J. Mao, *Nanomed.*, 2012, **7**, 1771–1784.
89 L. Pescosolido, W. Schuurman, J. Malda, P. Matricardi, F. Alhaique, T. Coviello, P. R. van Weeren, W. J. A. Dhert, W. E. Hennink and T. Vermonden, *Biomacromolecules*, 2011, **12**, 1831–1838.
90 L. Gasperini, J. F. Mano and R. L. Reis, *J. R. Soc., Interface*, 2014, **11**, 20140817.
91 A. Blaeser, D. F. Duarte Campos, M. Weber, S. Neuss, B. Theek, H. Fischer and W. Jahnen-Dechent, *BioRes. Open Access*, 2013, **2**, 374–384.
92 D. F. Duarte Campos, A. Blaeser, M. Weber, J. Jäkel, S. Neuss, W. Jahnen-Dechent and H. Fischer, *Biofabrication*, 2013, **5**, 015003.
93 F. Xu, B. Sridharan, N. G. Durmus, S. Wang, A. S. Yavuz, U. A. Gurkan and U. Demirci, *PLoS One*, 2011, **6**, e19344.
94 T. Dai, M. Tanaka, Y.-Y. Huang and M. R. Hamblin, *Expert Rev. Anti-Infect. Ther.*, 2011, **9**, 857–879.
95 A. Martínez-Ruvalcaba, E. Chornet and D. Rodrigue, *Carbohydr. Polym.*, 2007, **67**, 586–595.
96 F. Ahmadi, Z. Oveisi, S. M. Samani and Z. Amoozgar, *Res. Pharm. Sci.*, 2015, **10**, 1–16.
97 J. E. Arenas-Herrera, I. K. Ko, A. Atala and J. J. Yoo, *Biomed. Mater.*, 2013, **8**, 014106.
98 P. M. Crapo, T. W. Gilbert and S. F. Badylak, *Biomaterials*, 2011, **32**, 3233–3243.
99 F. Pati, J. Jang, D.-H. Ha, S. Won Kim, J.-W. Rhie, J.-H. Shim, D.-H. Kim and D.-W. Cho, *Nat. Commun.*, 2014, **5**, 3935.
100 F. Pati, D.-H. Ha, J. Jang, H. H. Han, J.-W. Rhie and D.-W. Cho, *Biomaterials*, 2015, **62**, 164–175.
101 A. Skardal, M. Devarasetty, H.-W. Kang, I. Mead, C. Bishop, T. Shupe, S. J. Lee, J. Jackson, J. Yoo, S. Soker and A. Atala, *Acta Biomater.*, 2015, **25**, 24–34.
102 C. S. Hughes, L. M. Postovit and G. A. Lajoie, *Proteomics*, 2010, **10**, 1886–1890.
103 J. E. Snyder, Q. Hamid, C. Wang, R. Chang, K. Emami, H. Wu and W. Sun, *Biofabrication*, 2011, **3**, 034112.
104 M. T. Poldervaart, H. Wang, J. van der Stok, H. Weinans, S. C. G. Leeuwenburgh, F. C. Öner, W. J. A. Dhert and J. Alblas, *PLoS One*, 2013, **8**, e72610.
105 L. Horváth, Y. Umehara, C. Jud, F. Blank, A. Petri-Fink and B. Rothen-Rutishauser, *Sci. Rep.*, 2015, **5**, 7974.
106 M. T. Poldervaart, H. Gremmels, K. van Deventer, J. O. Fledderus, F. C. Oner, M. C. Verhaar, W. J. A. Dhert and J. Alblas, *J. Controlled Release*, 2014, **184**, 58–66.
107 J. Zhu, *Biomaterials*, 2010, **31**, 4639–4656.
108 W. Li, P. Zhan, E. De Clercq, H. Lou and X. Liu, *Prog. Polym. Sci.*, 2013, **38**, 421–444.
109 J. G. Sathish, S. Sethu, M.-C. Bielsky, L. de Haan, N. S. French, K. Govindappa, J. Green, C. E. M. Griffiths, S. Holgate, D. Jones, I. Kimber, J. Moggs, D. J. Naisbitt, M. Pirmohamed, G. Reichmann, J. Sims, M. Subramanyam, M. D. Todd, J. W. Van Der Laan, R. J. Weaver and B. K. Park, *Nat. Rev. Drug Discovery*, 2013, **12**, 306–324.
110 A. Skardal, J. Zhang and G. D. Prestwich, *Biomaterials*, 2010, **31**, 6173–6181.
111 G. Gao, A. F. Schilling, T. Yonezawa, J. Wang, G. Dai and X. Cui, *Biotechnol. J.*, 2014, **9**, 1304–1311.
112 S. Hong, D. Sycks, H. F. Chan, S. Lin, G. P. Lopez, F. Guilak, K. W. Leong and X. Zhao, *Adv. Mater.*, 2015, **27**, 4035–4040.
113 F. Janvier, J. X. X. Zhu, J. Armstrong, H. J. Meiselman and G. Cloutier, *J. Mech. Behav. Biomed. Mater.*, 2013, **18**, 100–107.
114 N. C. Paxton, W. Smolan, T. Böck, F. P. W. Melchels, J. Groll and T. Juengst, *Biofabrication*, 2017, **9**(4), 044107.
115 A. Ribeiro, M. M. Blokzijl, R. Levato, C. W. Visser, M. Castilho, W. E. Hennink, T. Vermonden and J. Malda, *Biofabrication*, 2017, **10**(1), 014102.
116 K. Dubbin, A. Tabet and S. C. Heilshorn, *Biofabrication*, 2017, **9**, 044102.
117 M. Müller, J. Becher, M. Schnabelrauch and M. Zenobi-Wong, *Biofabrication*, 2015, **7**, 035006.
118 V. H. M. Mouser, A. Abbadessa, R. Levato, W. E. Hennink, T. Vermonden, D. Gawlitta and J. Malda, *Biofabrication*, 2017, **9**, 015026.
119 S. Stichler, T. Böck, N. C. Paxton, S. Bertlein, R. Levato, V. Schill, W. Smolan, J. Malda, J. Tessmar, T. Blunk and J. Groll, *Biofabrication*, 2017, **9**(4), 044108.

Published on 01 2018. Downloaded on 22.5.2025 22:31:12.

120 W. L. Ng, W. Y. Yeong and M. W. Naing, *Materials*, 2017, **10**(2), E190.
121 G. M. Cooper, E. D. Miller, G. E. Decesare, A. Usas, E. L. Lensie, M. R. Bykowski, J. Huard, L. E. Weiss, J. E. Losee and P. G. Campbell, *Tissue Eng., Part A*, 2010, **16**, 1749–1759.
122 F. Marga, K. Jakab, C. Khatiwala, B. Shepherd, S. Dorfman, B. Hubbard, S. Colbert and F. Gabor, *Biofabrication*, 2012, **4**, 022001.
123 C. Kucukgul, S. B. Ozler, I. Inci, E. Karakas, S. Irmak, D. Gozuacik, A. Taralp and B. Koc, *Biotechnol. Bioeng.*, 2015, **112**, 811–821.
124 K. Markstedt, A. Mantas, I. Tournier, H. Martínez Ávila, D. Hägg and P. Gatenholm, *Biomacromolecules*, 2015, **16**, 1489–1496.
125 M. Müller, E. Öztürk, Ø. Arlov, P. Gatenholm and M. Zenobi-Wong, *Ann. Biomed. Eng.*, 2017, **45**, 210–223.
126 H. Martínez Ávila, S. Schwarz, N. Rotter and P. Gatenholm, *Bioprinting*, 2016, **1**, 22–35.
127 K. Jakab, C. Norotte, B. Damon, F. Marga, A. Neagu, C. L. Besch-Williford, A. Kachurin, K. H. Church, H. Park, V. Mironov, R. Markwald, G. Vunjak-Novakovic and G. Forgacs, *Tissue Eng., Part A*, 2008, **14**, 413–421.
128 V. Mironov, R. P. Visconti, V. Kasyanov, G. Forgacs, C. J. Drake and R. R. Markwald, *Biomaterials*, 2009, **30**, 2164–2174.
129 C. A. Parzel, M. E. Pepper, T. Burg, R. E. Groff and K. J. L. Burg, *J. Tissue Eng. Regener. Med.*, 2009, **3**, 260–268.
130 C. M. Owens, F. Marga, G. Forgacs and C. M. Heesch, *Biofabrication*, 2013, **5**, 045007.
131 A. Faulkner-Jones, S. Greenhough, J. A. King, J. Gardner, A. Courtney and W. Shu, *Biofabrication*, 2013, **5**, 015013.
132 Z. Hajdu, V. Mironov, A. N. Mehesz, R. A. Norris, R. R. Markwald and R. P. Visconti, *J. Tissue Eng. Regener. Med.*, 2010, **4**, 659–664.
133 C. Norotte, F. S. Marga, L. E. Niklason and G. Forgacs, *Biomaterials*, 2009, **30**, 5910–5917.
134 M. E. Pepper, R. E. Groff, C. A. P. Cass, J. P. Mattimore, T. Burg and K. J. L. Burg, *Artif. Organs*, 2012, **36**, E151–E162.
135 M. S. Mannoor, Z. Jiang, T. James, Y. L. Kong, K. A. Malatesta, W. O. Soboyejo, N. Verma, D. H. Gracias and M. C. McAlpine, *Nano Lett.*, 2013, **13**, 2634–2639.
136 K. Buyukhatipoglu, R. Chang, W. Sun and A. M. Clyne, *Tissue Eng., Part C*, 2010, **16**, 631–642.
137 S. R. Shin, R. Farzad, A. Tamayol, V. Manoharan, P. Mostafalu, Y. S. Zhang, M. Akbari, S. M. Jung, D. Kim, M. Comotto, N. Annabi, F. E. Al-Hazmi, M. R. Dokmeci and A. Khademhosseini, *Adv. Mater.*, 2016, **28**, 3280–3289.
138 K. Zhu, S. R. Shin, T. van Kempen, Y.-C. Li, V. Ponraj, A. Nasajpour, S. Mandla, N. Hu, X. Liu, J. Leijten, Y.-D. Lin, M. A. Hussain, Y. S. Zhang, A. Tamayol and A. Khademhosseini, *Adv. Funct. Mater.*, 2017, **27**, 1605352.
139 S. V. Dorozhkin, *Acta Biomater.*, 2010, **6**, 715–734.
140 N. Roveri and M. Iafisco, *Nanotechnol. Sci. Appl.*, 2010, **3**, 107–125.
141 S. Catros, J.-C. Fricain, B. Guillotin, B. Pippenger, R. Bareille, M. Remy, E. Lebraud, B. Desbat, J. Amédée and F. Guillemot, *Biofabrication*, 2011, **3**, 025001.
142 F. Guillemot, A. Souquet, S. Catros, B. Guillotin, J. Lopez, M. Faucon, B. Pippenger, R. Bareille, M. Rémy, S. Bellance, P. Chabassier, J. C. Fricain and J. Amédée, *Acta Biomater.*, 2010, **6**, 2494–2500.
143 R. Goldman, *Adv. Skin Wound Care*, 2004, **17**, 24–35.
144 A. T. Grazul-Bilska, M. L. Johnson, J. J. Bilski, D. A. Redmer, L. P. Reynolds, A. Abdullah and K. M. Abdullah, *Drugs Today*, 2003, **39**, 787–800.
145 M. Atanasova and A. Whitty, *Crit. Rev. Biochem. Mol. Biol.*, 2012, **47**, 502–530.
146 E. D. Miller, J. A. Phillippi, G. W. Fisher, P. G. Campbell, L. M. Walker and L. E. Weiss, *Comb. Chem. High Throughput Screen.*, 2009, **12**, 604–618.
147 L. Elowsson, H. Kirsebom, V. Carmignac, B. Mattiasson and M. Durbeej, *Biomater. Sci.*, 2013, **1**, 402–410.
148 M. Gruene, M. Pflaum, A. Deiwick, L. Koch, S. Schlie, C. Unger, M. Wilhelmi, A. Haverich and B. N. Chichkov, *Biofabrication*, 2011, **3**, 015005.
149 R. El Assal, S. Guven, U. A. Gurkan, I. Gozen, H. Shafiee, S. Dalbeyler, N. Abdalla, G. Thomas, W. Fuld, B. M. W. Illigens, J. Estanislau, J. Khoory, R. Kaufman, C. Zylberberg, N. Lindeman, Q. Wen, I. Ghiran and U. Demirci, *Adv. Mater.*, 2014, **26**, 5815–5822.

 This journal is © The Royal Society of Chemistry 2018